2

# The protonmotive force and respiratory control

4

7

8             **MitoEAGLE Network**
9             Corresponding author: Gnaiger E
10             Contributing co-authors
11   Ahn B, Alves MG, Amati F, Aral C, Arandarčikaitė O, Åsander Frostner E, Bailey DM,
12   Bastos Sant'Anna Silva AC, Battino M, Beard DA, Ben-Shachar D, Bishop D, Breton S,
13   Brown GC, Brown RA, Buettner GR, Calabria E, Cardoso LHD, Carvalho E, Casado Pinna
14   M, Cervinkova Z, Chang SC, Chicco AJ, Chinopoulos C, Coen PM, Collins JL, Crisóstomo
15   L, Davis MS, Dias T, Distefano G, Doerrier C, Drahota Z, Duchen MR, Ehinger J, Elmer E,
16   Endlicher R, Fell DA, Ferko M, Ferreira JCB, Filipovska A, Fisar Z, Fisher J, Garcia-Roves
17   PM, Garcia-Souza LF, Genova ML, Gonzalo H, Goodpaster BH, Gorr TA, Grefte S, Han J,
18   Harrison DK, Hellgren KT, Hernansanz P, Holland O, Hoppel CL, Houstek J, Hunger M,
19   Iglesias-Gonzalez J, Irving BA, Iyer S, Jackson CB, Jansen-Dürr P, Jespersen NR, Jha RK,
20   Kaambre T, Kane DA, Kappler L, Karabatsiakis A, Keijer J, Keppner G, Komlodi T, Kopitar-
21   Jerala N, Krako Jakovljevic N, Kuang J, Kucera O, Labieniec-Watala M, Lai N, Laner V,
22   Larsen TS, Lee HK, Lemieux H, Lerfall J, Lucchinetti E, MacMillan-Crow LA, Makrecka-
23   Kuka M, Meszaros AT, Michalak S, Moisoi N, Molina AJA, Montaigne D, Moore AL,
24   Moreira BP, Mracek T, Muntane J, Muntean DM, Murray AJ, Nedergaard J, Nemec M,
25   Newsom S, Nozickova K, O'Gorman D, Oliveira PF, Oliveira PJ, Orynbayeva Z, Pak YK,
26   Palmeira CM, Patel HH, Pecina P, Pereira da Silva Grilo da Silva F, Pesta D, Petit PX,
27   Pichaud N, Pirkmajer S, Porter RK, Pranger F, Prochownik EV, Puurand M, Radenkovic F,
28   Reboredo P, Renner-Sattler K, Robinson MM, Rohlena J, Røsland GV, Rossiter HB,
29   Rybacka-Mossakowska J, Salvadego D, Scatena R, Schartner M, Scheibye-Knudsen M,
30   Schilling JM, Schlattner U, Schoenfeld P, Scott GR, Shabalina IG, Shevchuk I, Siewiera K,
31   Singer D, Sobotka O, Spinazzi M, Stankova P, Stier A, Stocker R, Sumbalova Z, Suravajhala
32   P, Tanaka M, Tandler B, Tepp K, Tomar D, Towheed A, Tretter L, Trivigno C, Tronstad KJ,
33   Trougakos IP, Tyrrell DJ, Urban T, Velika B, Vendelin M, Vercesi AE, Victor VM, Villena
34   JA, Wagner BA, Ward ML, Watala C, Wei YH, Wieckowski MR, Wohlwend M, Wolff J,
35            Wuest RCI, Zaugg K, Zaugg M, Zorzano A

36

37             Supporting co-authors:
38   Bakker BM, Bernardi P, Boetker HE, Borsheim E, Borutaitė V, Bouitbir J, Calbet JA, Calzia
39   E, Chaurasia B, Clementi E, Coker RH, Collin A, Das AM, De Palma C, Dubouchaud H,
40   Durham WJ, Dyrstad SE, Engin AB, Fornaro M, Gan Z, Garlid KD, Garten A, Gourlay CW,
41   Granata C, Haas CB, Haavik J, Haendeler J, Hand SC, Hepple RT, Hickey AJ, Hoel F, Jang
42   DH, Kainulainen H, Khamoui AV, Klingenspor M, Koopman WJH, Kowaltowski AJ,
43   Krajcova A, Lane N, Lenaz G, Malik A, Markova M, Mazat JP, Menze MA, Methner A,
44   Neuzil J, Oliveira MT, Pallotta ML, Parajuli N, Pettersen IKN, Porter C, Pulinilkunnil T,
45   Ropelle ER, Salin K, Sandi C, Sazanov LA, Silber AM, Skolik R, Smenes BT, Soares FAA,
46   Sokolova I, Sonkar VK, Swerdlow RH, Szabo I, Trifunovic A, Thyfault JP, Valentine JM,
47            Vieyra A, Votion DM, Williams C, Zischka H

48

51

Correspondence: Gnaiger E

*Department of Visceral, Transplant and Thoracic Surgery, D. Swarovski Research Laboratory, Medical University of Innsbruck, Innrain 66/4, A-6020 Innsbruck, Austria*

*Email:* erich.gnaiger@i-med.ac.at

*Tel: +43 512 566796, Fax: +43 512 566796 20*

*This manuscript on 'The protonmotive force and respiratory control' is a position statement in the frame of COST Action CA15203 MitoEAGLE. The list of co-authors evolved beyond **phase 1** (phase 1 versions 1-44) in the **bottom-up** spirit of COST.*

*This is an open invitation to scientists and students to join as co-authors, to provide a balanced view on mitochondrial respiratory control, a fundamental introductory presentation of the concept of the protonmotive force, and a consensus statement on reporting data of mitochondrial respiration in terms of metabolic flows and fluxes.*

*Mitochondrial fitness mapping - Quality management network*
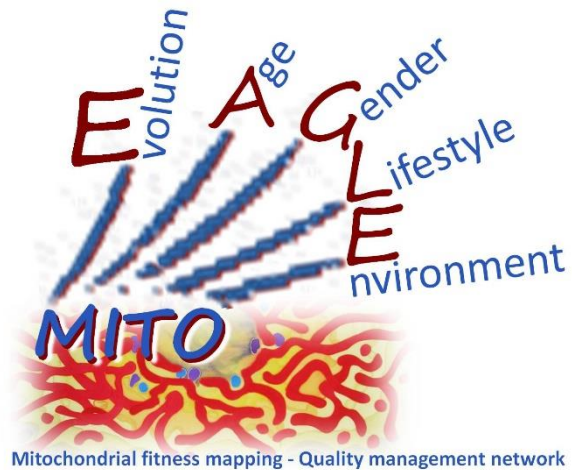
*   ***Phase 2:** MitoEAGLE preprint (Versions 01 – 16): We continue to invite comments and suggestions, particularly if you are an **early career investigator adding an open future-oriented perspective**, or an **established scientist providing a balanced historical basis**. Your critical input into the quality of the manuscript will be most welcome, improving our aims to be educational, general, consensus-oriented, and practically helpful for students working in mitochondrial respiratory physiology.*

*   ***Phase 3 (2017-11-11) Print version forMiP2017 and MitoEAGLE workshop in Hradec Kralove:***

*» http://www.mitoeagle.org/index.php/MiP2017_Hradec_Kralove_CZ*

***Discussion of manuscript submission to a preprint server, such as BioRxiv; invite further opinion leaders:** To join as a co-author, please feel free to focus on a particular section in terms of direct input and references, contributing to the scope of the manuscript from the perspective of your expertise. Your comments will be largely posted on the discussion page of the MitoEAGLE preprint website.*

*If you prefer to submit comments in the format of a referee's evaluation rather than a contribution as a co-author, I will be glad to distribute your views to the updated list of co-authors for a balanced response. We would ask for your consent on this open bottom-up policy.*

***Phase 4:** Journal submission. We plan a series of follow-up reports by the expanding MitoEAGLE Network, to increase the scope of recommendations on harmonization and facilitate global communication and collaboration. Further discussions: MitoEAGLE Working Group Meetings, various conferences (EBEC 2018 in Budapest).*

*I thank you in advance for your feedback.*
*With best wishes,*

*Erich Gnaiger*

*Chair Mitochondrial Physiology Society  - http://www.mitophysiology.org*
*Chair COST Action MitoEAGLE - http://www.mitoeagle.org*

**Contents**

**Abstract** Clarity of concept and consistency of nomenclature are key trademarks of a research field. These trademarks facilitate effective transdisciplinary communication, education, and ultimately further discovery. As the knowledge base and importance of mitochondrial physiology to human health expand, the necessity for harmonizing nomenclature concerning mitochondrial respiratory states and rates has become increasingly apparent. Peter Mitchell's chemiosmotic theory establishes the links between electric and chemical components of energy transformation and coupling in oxidative phosphorylation. The unifying concept of the protonmotive force provides the framework for developing a consistent theory and nomenclature for mitochondrial physiology and bioenergetics. Herein, we follow IUPAC guidelines on general terms of physical chemistry, extended by considerations on open systems and irreversible thermodynamics. The protonmotive force is not a vector force as defined in physics. This conflict is resolved by the generalized formulation of isomorphic, compartmental forces in energy transformations. We align the nomenclature and symbols of classical bioenergetics with a concept-driven constructive terminology to express the meaning of each quantity clearly and consistently. Uniform standards for evaluation of respiratory states and rates will ultimately support the development of databases of mitochondrial respiratory function in species, tissues, and cells studied under diverse physiological and experimental conditions. In this position statement, in the frame of COST Action MitoEAGLE, we endeavour to provide a balanced view on mitochondrial respiratory control, a fundamentally updated presentation of the concept of the protonmotive force, and a critical discussion on reporting data of mitochondrial respiration in terms of metabolic flows and fluxes.

*Keywords:* Mitochondrial respiratory control, coupling control, mitochondrial preparations, protonmotive force, chemiosmotic theory, oxidative phosphorylation, OXPHOS, efficiency, electron transfer, ET; proton leak, LEAK, residual oxygen consumption, ROX, State 2, State 3, State 4, normalization, flow, flux

---

**Executive summary**

*In preparation.*

---

§**Note:** Subscript '§' indicates throughout the text those parts, where *potential differences* provide a mathematically correct but physicochemically incomplete description and should be replaced by *stoichiometric potential differences* (Gnaiger 1993b). A unified concept on vectorial motive transformations and scalar chemical reactions will be derived elsewhere (Gnaiger, in prep.). Appreciation of the fundamental distinction between *differences of potential* versus *differences of stoichiometric potential* may be considered a key to critically evaluate the arguments presented in Section 3 on the protonmotive force. Since this discussion appears to be presently beyond the scope of a MitoEAGLE position statement, Section 3 will be removed from the next version and final manuscript. This section should become a topic of discussion within Working Group 1 of the MitoEAGLE consortium, following a primary peer-reviewed publication of the concept of stoichiometric potential differences.

<div align="center">

**Next version:**
http://www.mitoeagle.org/index.php/MitoEAGLE_preprint_2018-02-08

</div>

204

**Box 1:**

**In brief: Mitochondria and Bioblasts**

- Does the public expect biologists to understand Darwin's theory of evolution?
- Do students expect that researchers of bioenergetics can explain Mitchell's theory of chemiosmotic energy transformation?

**Mitochondria** are the oxygen-consuming electrochemical generators which evolved from endosymbiotic bacteria (Margulis 1970; Lane 2005). They were described by Richard Altmann (1894) as 'bioblasts', which include not only the mitochondria as presently defined, but also symbiotic and free-living bacteria. The word 'mitochondria' (Greek mitos: thread; chondros: granule) was introduced by Carl Benda (1898).

Mitochondrial dysfunction is associated with a wide variety of genetic and degenerative diseases. Robust mitochondrial function is supported by physical exercise and caloric balance, and is central for sustained metabolic health throughout life. Therefore, a more consistent presentation of mitochondrial physiology will improve our understanding of the etiology of disease, the diagnostic repertoire of mitochondrial medicine, with a focus on protective medicine, lifestyle and healthy aging.

We now recognize mitochondria as dynamic organelles with a double membrane that are contained within eukaryotic cells. The mitochondrial inner membrane (mtIM) shows dynamic tubular to disk-shaped cristae that separate the mitochondrial matrix, *i.e.*, the negatively charged internal mitochondrial compartment, and the intermembrane space; the latter being positively charged and enclosed by the mitochondrial outer membrane (mtOM). The mtIM contains the non-bilayer phospholipid cardiolipin, which is not present in any other eukaryotic cellular membrane. Cardiolipin promotes the formation of respiratory supercomplexes, which are supramolecular assemblies based upon specific, though dynamic, interactions between individual respiratory complexes (Greggio *et al.* 2017; Lenaz *et al.* 2017). Membrane fluidity is an important parameter influencing functional properties of proteins incorporated in the membranes (Waczulikova *et al.* 2007).

Mitochondria are the structural and functional elements of cell respiration. Cell respiration is the consumption of oxygen by electron transfer coupled to electrochemical proton translocation across the mtIM. In the process of oxidative phosphorylation (OXPHOS), the reduction of $O_2$ is electrochemically coupled to the transformation of energy in the form of adenosine triphosphate (ATP; Mitchell 1961, 2011). Mitochondria are the powerhouses of the cell which contain the machinery of the OXPHOS-pathways, including transmembrane respiratory complexes (*i.e.*, proton pumps with FMN, Fe-S and cytochrome $b$, $c$, $aa_3$ redox systems); alternative dehydrogenases and oxidases; the coenzyme ubiquinone (Q); F-ATPase or ATP synthase; the enzymes of the tricarboxylic acid cycle and the fatty acid oxidation enzymes; transporters of ions, metabolites and co-factors; and mitochondrial kinases related to energy transfer pathways. The mitochondrial proteome comprises over 1,200 proteins (Calvo *et al.* 2015; 2017), mostly encoded by nuclear DNA (nDNA), with a variety of functions, many of which are relatively well known (*e.g.* apoptosis-regulating proteins), while others are still under investigation, or need to be identified (*e.g.* alanine transporter).

There is a constant crosstalk between mitochondria and the other cellular components, maintaining cellular mitostasis through regulation at both the transcriptional and post-translational level, and through cell signalling including proteostatic (e.g. the ubiquitin-proteasome and autophagy-lysosome pathways) and genome stability modules throughout the cell cycle or even cell death, contributing to homeostatic regulation in response to varying energy demands and stress (Quiros *et al.* 2016). In addition to mitochondrial movement along the microtubules, mitochondrial morphology can change in response to energy requirements of the cell via processes known as fusion and fission, through which mitochondria communicate

within a network, and in response to intracellular stress factors causing swelling and ultimately permeability transition.

Mitochondria typically maintain several copies of their own genome (hundred to thousands per cell; Cummins 1998), which is maternally inherited (White *et al.* 2008) and known as mitochondrial DNA (mtDNA). One exception to strictly maternal inheritance in animals is found in bivalves (Breton *et al.* 2007). mtDNA is 16.5 kB in length, contains 13 protein-coding genes for subunits of the transmembrane respiratory Complexes CI, CIII, CIV and F-ATPase, and also encodes 22 tRNAs and the mitochondrial 16S and 12S rRNA. Additional gene content is encoded in the mitochondrial genome, *e.g.* microRNAs, piRNA, smithRNAs, repeat associated RNA, and even additional proteins (Duarte *et al.* 2014; Lee *et al.* 2015; Cobb *et al.* 2016). The mitochondrial genome is both regulated and supplemented by nuclear-encoded mitochondrial targeted proteins.

Abbreviation: mt, as generally used in mtDNA. Mitochondrion is singular and mitochondria is plural.

'*For the physiologist, mitochondria afforded the first opportunity for an experimental approach to structure-function relationships, in particular those involved in active transport, vectorial metabolism, and metabolic control mechanisms on a subcellular level*' (Ernster and Schatz 1981).

## 1. Introduction

Mitochondria are the powerhouses of the cell with numerous physiological, molecular, and genetic functions (**Box 1**). Every study of mitochondrial function and disease is faced with **E**volution, **A**ge, **G**ender and sex, **L**ifestyle, and **E**nvironment (EAGLE) as essential background conditions intrinsic to the individual patient or subject, cohort, species, tissue and to some extent even cell line. As a large and highly coordinated group of laboratories and researchers, the mission of the global MitoEAGLE Network is to generate the necessary scale, type, and quality of consistent data sets and conditions to address this intrinsic complexity. Harmonization of experimental protocols and implementation of a quality control and data management system are required to interrelate results gathered across a spectrum of studies and to generate a rigorously monitored database focused on mitochondrial respiratory function. In this way, researchers within the same and across different disciplines will be positioned to compare findings across traditions and generations to an agreed upon set of clearly defined and accepted international standards.

Reliability and comparability of quantitative results depend on the accuracy of measurements under strictly-defined conditions. A conceptual framework is required to warrant meaningful interpretation and comparability of experimental outcomes carried out by research groups at different institutes. With an emphasis on quality of research, collected data can be useful far beyond the specific question of a particular experiment. Enabling meta-analytic studies is the most economic way of providing robust answers to biological questions (Cooper *et al.* 2009). Vague or ambiguous jargon can lead to confusion and may relegate valuable signals to wasteful noise. For this reason, measured values must be expressed in standardized units for each parameter used to define mitochondrial respiratory function. Standardization of nomenclature and definition of technical terms are essential to improve the awareness of the intricate meaning of current and past scientific vocabulary, for documentation and integration into databases in general, and quantitative modelling in particular (Beard 2005). The focus on the protonmotive force, coupling states, and fluxes through metabolic pathways of aerobic energy transformation in mitochondrial preparations is a first step in the attempt to generate a harmonized and conceptually-oriented nomenclature in bioenergetics and mitochondrial physiology. The protonmotive force is a potential difference[§], $\Delta p$, and thus is not a force as defined in physics. Therefore, a detailed formal treatment is warranted of isomorphic forces

306  and fluxes in bioenergetics. Coupling states of intact cells and respiratory control by fuel
307  substrates and specific inhibitors of respiratory enzymes will be reviewed in subsequent
308  communications.
309
310
311  **2. Oxidative phosphorylation and coupling states in mitochondrial preparations**
312    *'Every professional group develops its own technical jargon for talking about matters of*
313    *critical concern ... People who know a word can share that idea with other members of*
314    *their group, and a shared vocabulary is part of the glue that holds people together and*
315    *allows them to create a shared culture'* (Miller 1991).
316
317    **Mitochondrial preparations** are defined as either isolated mitochondria, or tissue and
318  cellular preparations in which the barrier function of the plasma membrane is disrupted. The
319  plasma membrane separates the cytosol, nucleus, and organelles (the intracellular
320  compartment) from the environment of the cell. The plasma membrane consists of a lipid
321  bilayer, embedded proteins, and attached organic molecules that collectively control the
322  selective permeability of ions, organic molecules, and particles across the cell boundary. The
323  intact plasma membrane, therefore, prevents the passage of many water-soluble mitochondrial
324  substrates, such as succinate or adenosine diphosphate (ADP), that are required for the analysis
325  of respiratory capacity at kinetically-saturating concentrations, thus limiting the scope of
326  investigations into mitochondrial respiratory function in intact cells. The cholesterol content of
327  the plasma membrane is high compared to mitochondrial membranes. Therefore, mild
328  detergents, such as digitonin and saponin, can be applied to selectively permeabilize the plasma
329  membrane by interaction with cholesterol and allow free exchange of cytosolic components
330  with ions and organic molecules of the immediate cell environment, while maintaining the
331  integrity and localization of organelles, cytoskeleton, and the nucleus. Application of optimum
332  concentrations of permeabilization agents (mild detergents or toxins) leads to the complete loss
333  of cell viability, tested by nuclear staining and washout of cytosolic marker enzymes such as
334  lactate dehydrogenase, while mitochondrial function remains intact. The respiration rate of
335  isolated mitochondria remains unaltered after the addition of low concertations of digitonin or
336  saponin. In addition to mechanical permeabilization during homogenization of tissue,
337  peremeabilization agents may be applied to ensure permeabilization of all cells. Suspensions of
338  cells permeabilized in the respiration chamber and crude tissue homogenates contain all
339  components of the cell at highly diluted concentrations. All mitochondria are retained in
340  chemically-permeabilized mitochondrial preparations and crude tissue homogenates. In the
341  preparation of isolated mitochondria, the cells or tissues are homogenized, and the mitochondria
342  are separated from other cell fractions and purified by differential centrifugation, entailing the
343  loss of a fraction of mitochondria. Typical mitochondrial recovery ranges from 30% to 80%.
344  Maximization of the purity of isolated mitochondria may compromise not only the
345  mitochondrial yield but also the structural and functional integrity. Therefore, protocols for
346  isolation of mitochondria need to be optimized according to the relevant questions addressed in
347  a study. The term mitochondrial preparation does not include further fractionation of
348  mitochondrial components, as well as submitochondrial particles.
349
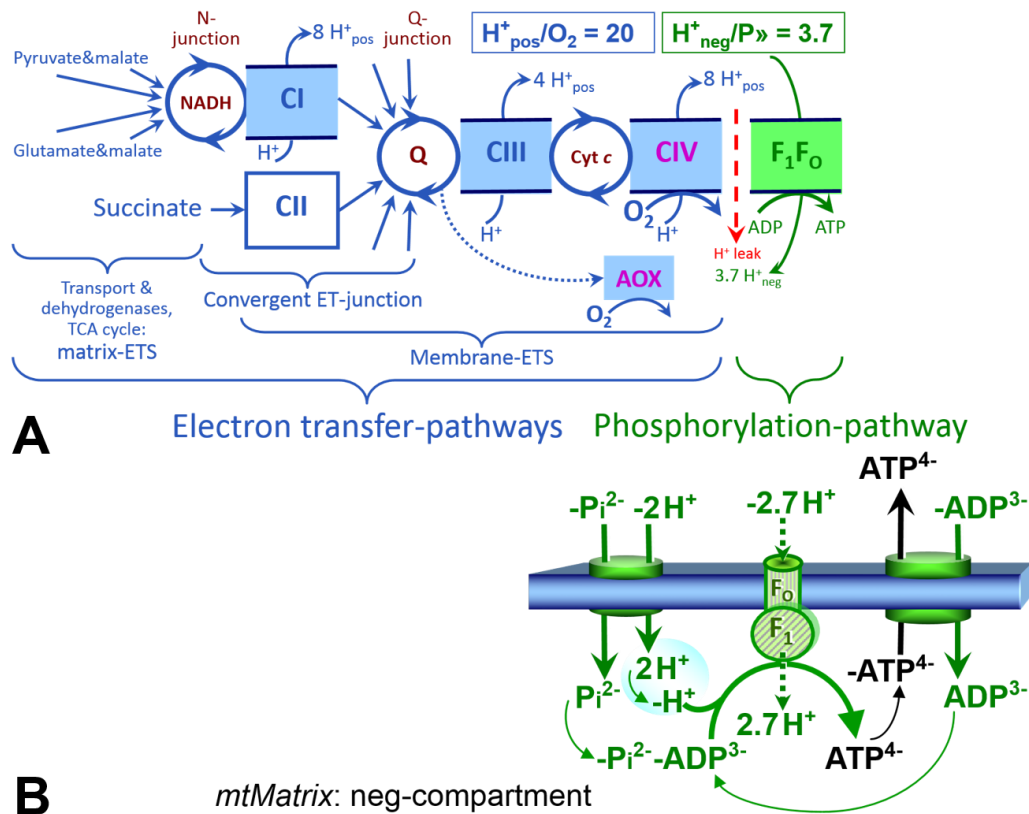
**Fig. 1. The oxidative phosphorylation (OXPHOS) system. (A)** The mitochondrial electron transfer system (ETS) is fuelled by diffusion and transport of substrates across the mtOM and mtIM and consists of the matrix-ETS and membrane-ETS. Electron transfer (ET) pathways are coupled to the phosphorylation-pathway. ET-pathways converge at the N-junction and Q-junction (additional arrows indicate electron entry into the Q-junction through electron transferring flavoprotein, glycerophosphate dehydrogenase, dihydro-orotate dehydrogenase, choline dehydrogenase, and sulfide-ubiquinone oxidoreductase). The dotted arrow indicates the branched pathway of oxygen consumption by alternative quinol oxidase (AOX). The $H^+_{pos}/O_2$ ratio is the outward proton flux from the matrix space to the positively (pos) charged compartment, divided by catabolic $O_2$ flux in the NADH-pathway. The $H^+_{neg}/P»$ ratio is the inward proton flux from the inter-membrane space to the negatively (neg) charged matrix space, divided by the flux of phosphorylation of ADP to ATP (Eq. 1). Due to ion leaks and proton slip these are not fixed stoichiometries. **(B)** Phosphorylation-pathway catalyzed by the proton pump $F_1F_O$-ATPase, adenine nucleotide translocase, and inorganic phosphate transporter. The $H^+_{neg}/P»$ stoichiometry is the sum of the coupling stoichiometry in the F-ATPase reaction (-2.7 $H^+_{pos}$ from the positive intermembrane space, 2.7 $H^+_{neg}$ to the matrix, *i.e.*, the negative compartment) and the proton balance in the translocation of $ADP^{2-}$, $ATP^{3-}$ and $P_i^{2-}$. Modified from (A) Lemieux *et al.* (2017) and (B) Gnaiger (2014).

*2.1. Three coupling states of mitochondrial preparations and residual oxygen consumption*

**Respiratory capacities in coupling control states:** To extend the classical nomenclature on mitochondrial coupling states (Section 2.3) by a concept-driven terminology that incorporates explicitly information on the nature of respiratory states, the terminology must be general and not restricted to any particular experimental protocol or mitochondrial preparation (Gnaiger 2009). We focus primarily on the conceptual 'why', along with clarification of the experimental 'how'. In the following section, the concept-driven terminology is explained and coupling states are defined. We define respiratory capacities, comparable to channel capacity

378 in information theory (Schneider 2006), as the upper bound of the rate of respiration measured
379 in defined coupling control states and electron transfer-pathway (ET-pathway) states.

380 To provide a diagnostic reference for respiratory capacities of core energy metabolism,
381 the capacity of *oxidative phosphorylation*, OXPHOS, is measured at kinetically-saturating
382 concentrations of ADP and inorganic phosphate, $P_i$. The *oxidative* ET-capacity reveals the
383 limitation of OXPHOS-capacity mediated by the *phosphorylation*-pathway. The ET- and
384 phosphorylation-pathways comprise coupled segments of the OXPHOS-system. ET-capacity
385 is measured as noncoupled respiration by application of *external uncouplers*. The contribution
386 of *intrinsically uncoupled* oxygen consumption is most easily studied in the absence of ADP,
387 *i.e.*, by not stimulating phosphorylation, or by inhibition of the phosphorylation-pathway. The
388 corresponding states are collectively classified as LEAK-states, when oxygen consumption
389 compensates mainly for ion leaks including the proton leak (**Table 1**). Defined coupling states
390 are induced by: (*1*) adding cation chelators such as EGTA, binding free $Ca^{2+}$ and thus limiting
391 cation cycling; (*2*) adding ADP and $P_i$; (*3*) inhibiting the phosphorylation-pathway; and (*4*)
392 uncoupler titrations, while maintaining a defined ET-pathway state with constant fuel substrates
393 and inhibitors of specific branches of the ET-pathway (**Fig. 1**).

394

395 **Table 1. Coupling states and residual oxygen consumption in mitochondrial**
396 **preparations in relation to respiration- and phosphorylation-rate, $J_{kO_2}$ and $J_{P»}$,**
397 **and protonmotive force, $\Delta_m F_{H+}$. Coupling states are established at kinetically-**
398 **saturating concentrations of fuel substrates and $O_2$.**

| State | $J_{kO_2}$ | $J_{P»}$ | $\Delta_m F_{H+}$ | Inducing factors | Limiting factors |
|---|---|---|---|---|---|
| LEAK | $L$; low, cation leak-dependent respiration | 0 | max. | proton leak, slip, and cation cycling | $J_{P»} = 0$: (*1*) without ADP, $L_N$; (*2*) max. ATP/ADP ratio, $L_T$; or (*3*) inhibition of the phosphorylation-pathway, $L_{Omy}$ |
| OXPHOS | $P$; high, ADP-stimulated respiration | max. | high | kinetically-saturating [ADP] and [$P_i$] | $J_{P»}$ by phosphorylation-pathway; or $J_{kO_2}$ by ET-capacity |
| ET | $E$; max., noncoupled respiration | 0 | low | optimal external uncoupler concentration for max. $J_{O_2,E}$ | $J_{kO_2}$ by ET-capacity |
| ROX | $Rox$; min., residual $O_2$ consumption | 0 | 0 | $J_{O_2,Rox}$ in non-ET-pathway oxidation reactions | full inhibition of ET-pathway; or absence of fuel substrates |

399

400 **Kinetic control:** Coupling control states are established in the study of mitochondrial
401 preparations to obtain reference values for various output variables. Physiological conditions *in*
402 *vivo* deviate from these experimentally obtained states. Since kinetically-saturating
403 concentrations, *e.g.* of ADP or oxygen, may not apply to physiological intracellular conditions,
404 relevant information is obtained in studies of kinetic responses to conditions intermediate
405 between the LEAK state at zero [ADP] and the OXPHOS-state at saturating [ADP], or of
406 respiratory capacities in the range between kinetically-saturating [$O_2$] and anoxia (Gnaiger
407 2001).

408      **The steady-state:** Mitochondria represent a thermodynamically open system in non-
409 equilibrium states of biochemical energy transformation. State variables (protonmotive force;
410 redox states) and metabolic *rates* (fluxes) are measured in defined mitochondrial respiratory
411 *states*. Strictly, steady states can be obtained only in open systems, in which changes by *internal*
412 transformations, *e.g.*, $O_2$ consumption, are instantaneously compensated for by *external* fluxes,
413 *e.g.*, $O_2$ supply, such that oxygen concentration does not change in the system (Gnaiger 1993b).
414 Mitochondrial respiratory states monitored in closed systems satisfy the criteria of pseudo-
415 steady states for limited periods of time, when changes in the system (concentrations of $O_2$,
416 fuel substrates, ADP, $P_i$, $H^+$) do not exert significant effects on metabolic fluxes (respiration,
417 phosphorylation). Such pseudo-steady states require respiratory media with sufficient buffering
418 capacity and kinetically-saturating concentrations of substrates to be maintained, and thus
419 depend on the kinetics of the processes under investigation.

420      **Specification of biochemical dose:** Substrates, uncouplers, inhibitors, and other
421 biochemical reagents are titrated to dissect mitochondrial function. Nominal concentrations of
422 these substances are usually reported as initial amount of substance concentration [mol·L$^{-1}$] in
423 the incubation medium. When aiming at the measurement of kinetically saturated processes
424 such as OXPHOS-capacities, the concentrations for substrates can be chosen in light of the
425 apparent equilibrium constant, $K_m$'. In the case of hyperbolic kinetics, only 80% of maximum
426 respiratory capacity is obtained at a substrate concentration of four times the $K_m$', whereas
427 substrate concentrations of 5, 9, 19 and 49 times the $K_m$' are theoretically required for reaching
428 83%, 90%, 95% or 98% of the maximal rate (Gnaiger 2001). Other reagents are chosen to
429 inhibit or alter some process. The amount of these chemicals in an experimental incubation is
430 selected to maximize effect, yet not lead to unacceptable off-target consequences that would
431 adversely affect the data being sought. Specifying the amount of substance in an incubation as
432 nominal concentration in the aqueous incubation medium can be ambiguous (Doskey *et al*.
433 2015), particularly when lipophilic substances (oligomycin; uncouplers, permeabilization
434 agents) or cations (TPP$^+$; fluorescent dyes such as safranin, TMRM) are applied which
435 accumulate in biological membranes or the mitochondrial matrix. For example, a dose of
436 digitonin of 8 fmol·cell$^{-1}$ (10 μg·10$^{-6}$ cells) is optimal for permeabilization of endothelial cells,
437 and the concentration in the incubation medium has to be adjusted according to the cell density
438 applied (Doerrier *et al*. 2018). Generally, dose/exposure can be specified per unit of biological
439 sample, *i.e.*, (nominal moles of xenobiotic)/(number of cells) [mol·cell$^{-1}$] or, as appropriate, per
440 mass of biological sample [mol·kg$^{-1}$]. This approach to specification of dose/exposure provides
441 a scalable parameter that can be used to design experiments, help interpret a wide variety of
442 experimental results, and provide absolute information that allows researchers worldwide to
443 make the most use of published data (Doskey *et al*. 2015).

444      **Phosphorylation, P»:** *Phosphorylation* in the context of OXPHOS is defined as
445 phosphorylation of ADP by $P_i$ to ATP. On the other hand, the term phosphorylation is used
446 generally in many different contexts, *e.g.* protein phosphorylation. This justifies consideration
447 of a symbol more discriminating and specific than P as used in the P/O ratio (phosphate to
448 atomic oxygen ratio; O = 0.5 $O_2$), where P indicates phosphorylation of ADP to ATP or GDP
449 to GTP. We propose the symbol P» for the endergonic (uphill) direction of phosphorylation
450 ADP→ATP, and likewise the symbol P« for the corresponding exergonic (downhill) hydrolysis
451 ATP→ADP (**Fig. 2**). P» refers mainly to electrontransfer phosphorylation but may also involve
452 substrate-level phosphorylation as part of the tricarboxylic acid cycle (succinyl-CoA ligase)
453 and phosphorylation of ADP catalyzed by phosphoenolpyruvate carboxykinase.
454 Transphosphorylation is performed by adenylate kinase, creatine kinase, hexokinase and
455 nucleoside diphosphate kinase. In isolated mammalian mitochondria ATP production catalyzed
456 by adenylate kinase, 2 ADP ↔ ATP + AMP, proceeds without fuel substrates in the presence
457 of ADP (Komlódi and Tretter 2017). Kinase cycles are involved in intracellular energy transfer
458 and signal transduction for regulation of energy flux.
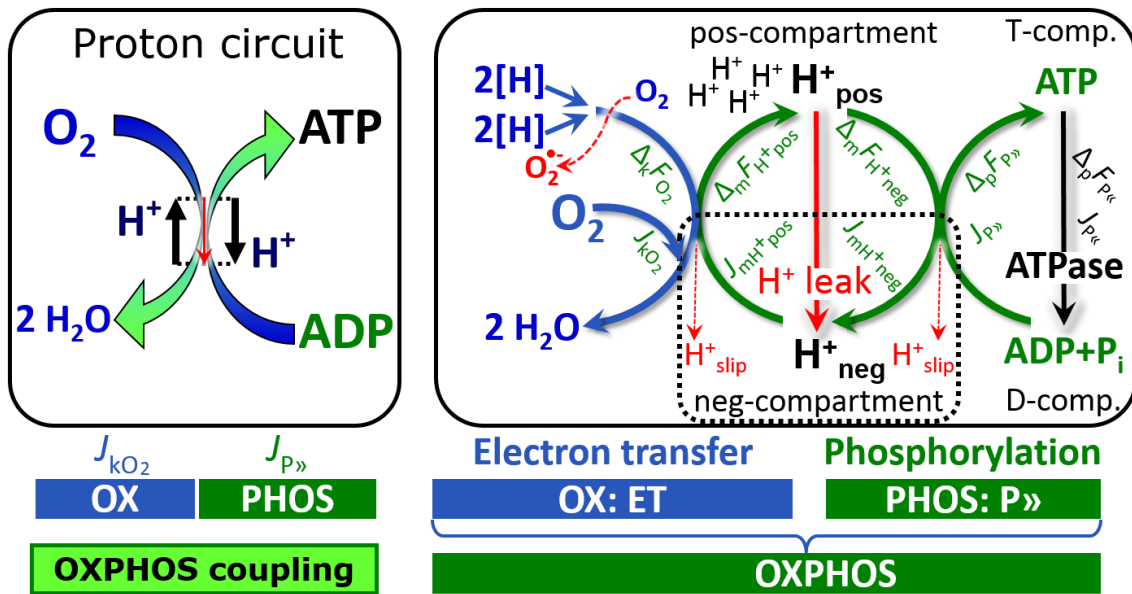
**Fig. 2. The proton circuit and coupling in oxidative phosphorylation (OXPHOS).** Oxygen flux, $J_{kO_2}$, through the catabolic ET-pathway, k, is coupled to flux through the phosphorylation-pathway of ADP to ATP, $J_{P»}$. The proton pumps of the ET-pathway drive proton flux into the positive (pos) compartment, $J_{mH+pos}$, which generates the output protonmotive force, $\Delta_m F_{H+pos}$. F-ATPase is coupled to inward proton current into the negative (neg) compartment, $J_{mH+neg}$, to phosphorylate ADP+$P_i$ to ATP, driven by the input protonmotive force, $\Delta_m F_{H+neg} = -\Delta_m F_{H+pos}$. 2[H] indicates the reduced hydrogen equivalents of fuel substrates that provide the chemical input force, $\Delta_k F_{O_2}$ [kJ/mol $O_2$], of the catabolic reaction k with oxygen (Gibbs energy of reaction per mole $O_2$ consumed in reaction k), typically in the range of -460 to -480 kJ/mol (1.2 V). The output force is given by the stoichiometric phosphorylation potential difference (ADP phosphorylated to ATP), $\Delta_p F_{P»}$, which varies *in vivo* ranging from about 48 to 62 kJ/mol under physiological conditions (Gnaiger 1993a). Fluxes are expressed per volume, $V$ [m$^3$], of the system. The system defined by the boundaries (full black line) is not a black box, but is analysed as a compartmental system. The negative compartment (neg-compartment, enclosed by the dotted line) is the matrix space, separated by the mtIM from the positive compartment (pos-compartment). ADP+$P_i$ and ATP are the substrate- and product-compartments (scalar ADP and ATP compartments, D-comp. and T-comp.), respectively. Chemical potentials of all substrates and products involved in the scalar reactions are measured in the pos-compartment for calculation of the scalar forces of reactions k and p, $\Delta_k F_{O_2}$ and $\Delta_p F_{P»} = -\Delta_p F_{P«}$. At steady-state proton turnover, $J_{\infty H+}$, and ATP turnover, $J_{\infty P}$, maintain a constant $\Delta_m F_{H+}$ and $\Delta_p F_{P»}$, when $J_{mH+\infty} = J_{mH+pos} = J_{mH+neg}$, and $J_{P\infty} = J_{P»} = J_{P«}$. Modified from Gnaiger (2014).

**Uncoupling:** Uncoupling is a general term comprising diverse mechanisms. Small differences of terms, *e.g.*, uncoupled *vs.* noncoupled, are easily overlooked, although they relate to different mechanisms of uncoupling (**Fig. 3**). An attempt at rigorous definition is required for clarification of concepts (**Table 2**).

1. Proton leak across the mtIM from the pos- to the neg-compartment (**Fig. 2**);
2. Cycling of other cations, strongly stimulated by permeability transition;
3. Proton slip in the proton pumps when protons are effectively not pumped (CI, CIII and CIV) or are not driving phosphorylation (F-ATPase);
4. Loss of compartmental integrity when electron transfer is acoupled;
5. Electron leak in the loosely coupled univalent reduction of oxygen ($O_2$; dioxygen) to superoxide anion radical ($O_2^{•-}$).
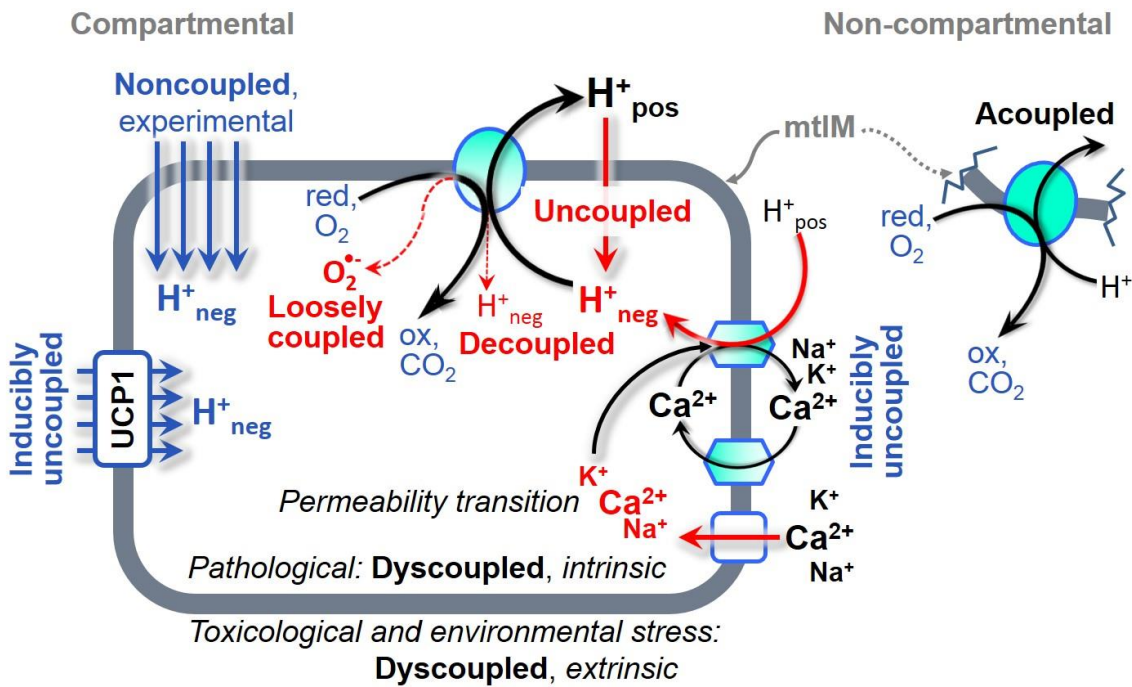
**Fig 3. Mechanisms of respiratory uncoupling.** An intact mitochondrial inner membrane, mtIM, is required for vectorial, compartmental coupling. 'Acoupled' respiration is the consequence of structural disruption with catalytic activity of non-compartmental mitochondrial fragments. Inducibly uncoupled (activation of UCP1) and experimentally noncoupled respiration (titration of protonophores) stimulate respiration to maximum oxygen flux of ET-capacity. Uncoupled, decoupled, and loosely coupled respiration are components of intrinsic LEAK respiration. Pathological dysfunction may affect all types of uncoupling, including permeability transition, causing intrinsically dyscoupled respiration. Similarly, toxicological and environmental stress factors can cause extrinsically dyscoupled respiration.

**LEAK-state** (**Fig. 4**): The LEAK-state is defined as a state of mitochondrial respiration when $O_2$ flux mainly compensates for ion leaks in the absence of ATP synthesis, at kinetically-saturating concentrations of $O_2$ and respiratory fuel substrates. LEAK-respiration is measured to obtain an estimate of *intrinsic uncoupling* without addition of an experimental uncoupler: (*1*) in the absence of adenylates; (*2*) after depletion of ADP at a maximum ATP/ADP ratio; or (*3*) after inhibition of the phosphorylation-pathway by inhibitors of F-



**Fig. 4. LEAK-state:** Phosphorylation is arrested, $J_{P_»} = 0$, and catabolic oxygen flux, $J_{kO_2,L}$, is controlled mainly by the proton leak, $J_{mH+neg,L}$, at maximum protonmotive force, $\Delta_m F_{H+pos}$. See also **Fig. 2** and **3**.

ATPase, such as oligomycin, or of adenine nucleotide translocase, such as carboxyatractyloside. It is important to consider adjustment of the nominal concentration of these inhibitors to the density of biological sample applied, to minimize or avoid inhibitory side-effects exerted on ET-capacity or even some dyscoupling.

**Table 2. Distinction of terms related to coupling and uncoupling (Fig. 3).**

| Term | Respiration | $P\gg/O_2$ | Note |
|---|---|---|---|
| acoupled |  | 0 | electron transfer in mitochondrial fragments without vectorial proton translocation |
| uncoupled | $L$ | 0 | non-phosphorylating intrinsic LEAK-respiration, without added protonophore |
| uncoupled |  | 0 | component of LEAK-respiration, uncoupled *sui generis*, ion diffusion across the mtIM |
| decoupled |  | 0 | component of LEAK-respiration, proton slip |
| loosely coupled |  | 0 | component of LEAK-respiration, lower coupling due to superoxide anion radical formation and bypass of proton pumps |
| dyscoupled |  | 0 | pathologically, toxicologically, environmentally increased uncoupling, mitochondrial dysfunction |
| inducibly uncoupled | $E$ | 0 | by UCP1 or cation (*e.g.* $Ca^{2+}$) cycling |
| noncoupled | $E$ | 0 | non-phosphorylating respiration stimulated to maximum flux at optimum exogenous uncoupler concentration (**Fig. 6**) |
| well-coupled | $P$ | high | phosphorylating respiration with an intrinsic LEAK component (**Fig. 5**) |
| fully coupled | $P - L$ | max. | OXPHOS-capacity corrected for LEAK-respiration (**Fig. 7**) |

**Proton leak and uncoupled respiration:** Proton leak is a leak current of protons. The intrinsic proton leak is the *uncoupled* process in which protons diffuse across the mtIM in the dissipative direction of the downhill protonmotive force without coupling to phosphorylation (**Fig. 4**). The proton leak flux depends non-linearly on the protonmotive force (Garlid *et al.* 1989; Divakaruni and Brand 2011), is a property of the mtIM, and may be enhanced due to possible contaminations by free fatty acids. Inducible uncoupling mediated by uncoupling protein 1 (UCP1) is physiologically controlled, *e.g.*, in brown adipose tissue. UCP1 is a member of the mitochondrial carrier family which is involved in the translocation of protons across the mtIM (Klingenberg 2017). As a consequence of this effective short-circuit, the protonmotive force diminishes, resulting in stimulation of electron transfer to $O_2$ and heat dissipation without phosphorylation of ADP.

**Cation cycling:** There can be other cation contributors to leak current including calcium and probably magnesium. Calcium current is balanced by mitochondrial $Na^+/Ca^{2+}$ exchange, which is balanced by $Na^+/H^+$ exchange or $K^+/H^+$ exchange. This is another effective uncoupling mechanism different from proton leak.

**Proton slip and decoupled respiration:** Proton slip is the *decoupled* process in which protons are only partially translocated by a proton pump of the ET-pathways and slip back to the original compartment. The proton leak is the dominant contributor to the overall leak current in mammalian mitochondria incubated under physiological conditions at 37 °C, whereas proton slip is increased at lower experimental temperature (Canton *et al.* 1995). Proton slip can also happen in association with the F-ATPase, in which case the proton slips downhill across the pump to the matrix without contributing to ATP synthesis. In each case, proton slip is a property of the proton pump and increases with the turnover rate of the pump.

552     **Electron leak and loosely coupled respiration**: Superoxide anion radical production by
553 the ETS leads to a bypass of proton pumps and correspondingly lower P»/$O_2$ ratio, which
554 depends on the actual site of electron leak and the scavenging of hydrogen peroxide by
555 cytochrome *c*, whereby electrons may re-enter the ETS with proton translocation by CIV.

556     **Loss of compartmental integrity and acoupled respiration:** Electron transfer and $O_2$
557 consumption proceed without compartmental proton translocation in disrupted mitochondrial
558 fragments. Such fragments form during mitochondrial isolation, and may not fully fuse to re-
559 establish structurally intact mitochondria. Loss of mtIM integrity, therefore, is the cause of
560 acoupled respiration, which is a nonvectorial dissipative process without control by the
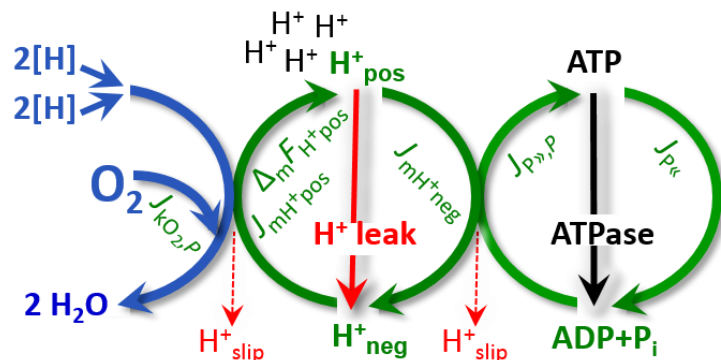561 protonmotive force.

562     **Dyscoupled respiration:** Mitochondrial injuries may lead to *dyscoupling* as a
563 pathological or toxicological cause of *uncoupled* respiration. Dyscoupling may involve any
564 type of uncoupling mechanism, *e.g.*, opening the permeability transition pore. Dyscoupled
565 respiration is distinguished from the experimentally induced *noncoupled* respiration in the ET-
566 state (**Fig. 3**).

567

568     **OXPHOS-state** (**Fig. 5**):
569 The OXPHOS-state is defined as
570 the respiratory state with
571 kinetically-saturating
572 concentrations of $O_2$, respiratory
573 and phosphorylation substrates,
574 and absence of exogenous
575 uncoupler, which provides an
576 estimate of the maximal
577 respiratory capacity in the
578 OXPHOS-state for any given ET-
579 pathway state. Respiratory
580 capacities at kinetically-saturating
581 substrate concentrations provide
582 reference values or upper limits of
583 performance, aiming at the
584 generation of data sets for



**Fig. 5. OXPHOS-state:** Phosphorylation, $J_{P»}$, is stimulated by kinetically-saturating [ADP] and inorganic phosphate, [$P_i$], and is supported by a high protonmotive force, $\Delta_m F_{H+pos}$. $O_2$ flux, $J_{kO_2,P}$, is well-coupled at a P»/$O_2$ ratio of $J_{P»,P}/J_{O_2,P}$. See also **Fig. 2**.

585 comparative purposes. Physiological activities and effects of substrate kinetics can be evaluated
586 relative to the OXPHOS-capacity.

587     As discussed previously, 0.2 mM ADP does not fully saturate flux in isolated
588 mitochondria (Gnaiger 2001; Puchowicz *et al*. 2004); greater ADP concentration is required,
589 particularly in permeabilized muscle fibres and cardiomyocytes, to overcome limitations by
590 intracellular diffusion and by the reduced conductance of the mtOM (Jepihhina *et al*. 2011,
591 Illaste *et al*. 2012, Simson *et al*. 2016), either through interaction with tubulin (Rostovtseva *et
592 al*. 2008) or other intracellular structures (Birkedal *et al*. 2014). In permeabilized muscle fibre
593 bundles of high respiratory capacity, the apparent $K_m$ for ADP increases up to 0.5 mM (Saks *et
594 al*. 1998), consistent with experimental evidence that >90% saturation is reached only at >5
595 mM ADP (Pesta and Gnaiger 2012). Similar ADP concentrations are also required for accurate
596 determination of OXPHOS-capacity in human clinical cancer samples and permeabilized cells
597 (Klepinin *et al*. 2016; Koit *et al*. 2017). Whereas 2.5 to 5 mM ADP is sufficient to obtain the
598 actual OXPHOS-capacity in many types of permeabilized tissue and cell preparations,
599 experimental validation is required in each specific case.

600

**Electron transfer-state** (**Fig. 6**): The ET-state is defined as the *noncoupled* state with kinetically-saturating concentrations of $O_2$, respiratory substrate and optimum *exogenous* uncoupler concentration for maximum $O_2$ flux, as an estimate of ET-capacity. Inhibition of respiration is observed at higher than optimum uncoupler concentrations. As a consequence of the nearly collapsed protonmotive force, the driving force is insufficient for phosphorylation, and $J_{P»} = 0$.
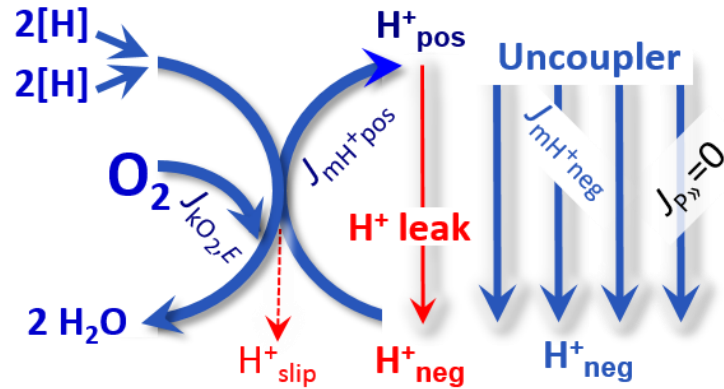


**Fig. 6. ET-state:** Noncoupled respiration, $J_{kO2,E}$, is maximum at optimum exogenous uncoupler concentration and phosphorylation is zero, $J_{P»} = 0$. See also Fig. 2.

Besides the three fundamental coupling states of mitochondrial preparations, the following respiratory state also is relevant to assess respiratory function:
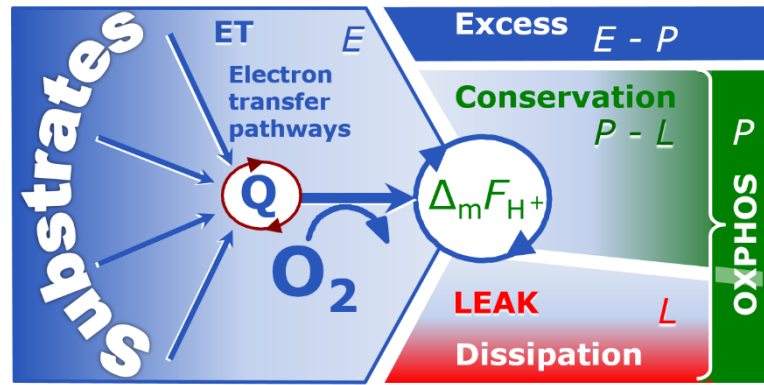
**ROX state and *Rox*:** The rate of residual oxygen consumption, *Rox*, is defined as $O_2$ consumption due to oxidative side reactions remaining after inhibition of ET, *e.g.*, with rotenone, malonic acid and antimycin A. Cyanide and azide not only inhibit CIV but several peroxidases which should be involved in *Rox*. ROX is not a coupling state. *Rox* represents a baseline that is used to correct mitochondrial respiration in defined coupling states. *Rox* is not necessarily equivalent to non-mitochondrial respiration, considering oxygen-consuming reactions in mitochondria not related to ET, such as oxygen consumption in reactions catalyzed by monoamine oxidases (type A and B), monooxygenases (cytochrome P450 monooxygenases), dioxygenase (sulfur dioxygenase and trimethyllysine dioxygenase), several hydoxylases, and more. Mitochondrial preparations, especially those obtained from liver, may be contaminated by peroxisomes. This fact makes the exact determination of mitochondrial oxygen consumption and mitochondria-associated generation of reactive oxygen species complicated (Schönfeld *et al.* 2009). The dependence of ROX-linked oxygen consumption needs to be studied in detail with respect to non-ET enzyme activities, availability of specific substrates, oxygen concentration, and electron leakage leading to the formation of reactive oxygen species.

*2.2. Coupling states and respiratory rates*

As an improvement of previous terminologies, we distinguish metabolic *pathways* from metabolic *states* and the corresponding metabolic *rates*; for example: ET-pathways (**Fig. 7**), ET-state (**Fig. 6**), and ET-capacity, $E$, respectively (**Table 1**). The protonmotive force is *high* in the OXPHOS-state when it drives phosphorylation, *maximum* in the LEAK-state of coupled mitochondria, driven by LEAK-respiration at a minimum back flux of cations to the matrix side, and *very low* in the ET-state when uncouplers short-circuit the proton cycle (**Table 1**).

The three coupling states, ET, LEAK and OXPHOS, are shown schematically with the corresponding respiratory rates, abbreviated as $E$, $L$ and $P$, respectively (**Fig. 7**).

**Fig. 7. Four-compartment model of oxidative phosphorylation.** Respiratory states (ET, OXPHOS, LEAK) and corresponding rates (*E, P, L*) are connected by the protonmotive force, $\Delta_m F_{H+}$. Electron transfer-capacity, *E*, is partitioned into (*1*) dissipative LEAK-respiration, *L*, when the Gibbs energy change of catabolic $O_2$ consumption is irreversibly lost, (*2*) net OXPHOS-capacity, *P-L*, with partial conservation of the capacity to perform work, and (*3*) the excess capacity, *E-P*. Modified from Gnaiger (2014).



*E* may exceed or be equal to *P*. *E > P* is observed in many types of mitochondria, varying between species, tissues and cell types (Gnaiger 2009). *E-P* is the excess ET-capacity pushing the phosphorylation-flux (**Fig. 1B**) to the limit of its *capacity of utilizing* the protonmotive force. In addition, the magnitude of *E-P* depends on the tightness of coupling or degree of uncoupling, since an increase of *L* causes *P* to increase towards the limit of *E*. The *excess E-P* capacity, *E-P*, therefore, provides a sensitive diagnostic indicator of specific injuries of the phosphorylation-pathway, under conditions when *E* remains constant but *P* declines relative to controls (**Fig. 7**). Substrate cocktails supporting simultaneous convergent electron transfer to the Q-junction for reconstitution of tricarboxylic acid cycle (TCA cycle or Krebs cycle) function establish pathway control states with high ET-capacity, and consequently increase the sensitivity of the *E-P* assay.

*E* cannot theoretically be lower than *P*. *E < P* must be discounted as an artefact, which may be caused experimentally by: (*1*) loss of oxidative capacity during the time course of the respirometric assay, since *E* is measured subsequently to *P*; (*2*) using insuffient uncoupler concentrations; (*3*) using high uncoupler concentrations which inhibit ET (Gnaiger 2008); (*4*) high oligomycin concentrations applied for measurement of *L* before titrations of uncoupler, when oligomycin exerts an inhibitory effect on *E*. On the other hand, the excess ET-capacity is overestimated if non-saturating [ADP] or [$P_i$] are used. See State 3 in the next section.

**P»/O₂ ratio:** The P»/$O_2$ ratio (P»/4 e⁻) is two times the 'P/O' ratio (P»/2 e⁻) of classical bioenergetics. P»/$O_2$ is a generalized symbol, independent of measurement of phosphorylation by determination of $P_i$ consumption ($P_i$/$O_2$ flux ratio), ADP depletion (ADP/$O_2$ flux ratio), or ATP production (ATP/$O_2$ flux ratio).

The mechanistic P»/$O_2$ ratio, which may be referred to also as P»/$O_2$ stoichiometry, is calculated from the proton-to-oxygen and proton-to-phosphorylation coupling stoichiometries (**Fig. 1A**),

$$\text{P»/O}_2 \;=\; \frac{\text{H}^+_{pos}/\text{O}_2}{\text{H}^+_{neg}/\text{P»}} \tag{1}$$

The H⁺$_{pos}$/$O_2$ *coupling stoichiometry* (referring to the full 4 electron reduction of $O_2$) depends on the ET-pathway control state which defines the relative involvement of the three coupling sites (CI, CIII and CIV) in the catabolic pathway of electrons to $O_2$. This varies with: (*1*) a bypass of CI by single or multiple electron input into the Q-junction; and (*2*) a bypass of CIV by involvement of AOX. H⁺$_{pos}$/$O_2$ is 12 in the ET-pathways involving CIII and CIV as proton pumps, increasing to 20 for the NADH-pathway (**Fig. 1A**), but a general consensus on H⁺$_{pos}$/$O_2$ stoichiometries remains to be reached (Hinkle 2005; Wikström and Hummer 2012; Sazanov

699     2015). The $H^+_{neg}/P»$ coupling stoichiometry (3.7; **Fig. 1A**) is the sum of 2.7 $H^+_{neg}$ required by
700     the F-ATPase of vertebrate and most invertebrate species (Watt *et al.* 2010) and the proton
701     balance in the translocation of ADP, ATP and $P_i$ (**Fig. 1B**). Taken together, the mechanistic
702     $P»/O_2$ ratio is calculated at 5.4 and 3.3 for NADH- and succinate-linked respiration, respectively
703     (Eq. 1). The corresponding classical P»/O ratios (referring to the 2 electron reduction of 0.5 $O_2$)
704     are 2.7 and 1.6 (Watt *et al.* 2010), in direct agreement with the measured P»/O ratio for succinate
705     of $1.58 \pm 0.02$ (Gnaiger *et al.* 2000).
706        The effective $P»/O_2$ flux ratio ($Y_{P»/O_2} = J_{P»}/J_{kO_2}$) is diminished relative to the mechanistic
707     $P»/O_2$ ratio by intrinsic and extrinsic uncoupling and dyscoupling (**Fig. 3**). Such generalized
708     uncoupling is different from switching to mitochondrial pathways that involve fewer than three
709     proton pumps ('coupling sites': Complexes CI, CIII and CIV), bypassing CI through multiple
710     electron entries into the Q-junction, or CIII and CIV through AOX (**Fig. 1**). Reprogramming of
711     mitochondrial pathways may be considered as a switch of gears (changing the stoichiometry)
712     rather than uncoupling (loosening the stoichiometry). In addition, $Y_{P»/O_2}$ depends on several
713     experimental conditions of flux control, increasing as a hyperbolic function of [ADP] to a
714     maximum value (Gnaiger 2001).
715        The net OXPHOS-capacity is calculated by subtracting *L* from *P* (**Fig. 7**). Then the net
716     $P»/O_2$ equals P»/(*P-L*), wherein the dissipative LEAK component in the OXPHOS-state may
717     be overestimated. This can be avoided by measuring LEAK-respiration in a state when the
718     protonmotive force is adjusted to its slightly lower value in the OXPHOS-state, *e.g.*, by titration
719     of an ET inhibitor (Divakaruni and Brand 2011). Any turnover-dependent components of
720     proton leak and slip, however, are underestimated under these conditions (Garlid *et al.* 1993).
721     In general, it is inappropriate to use the term *ATP production* or *ATP turnover* for the difference
722     of oxygen consumption measured in states *P* and *L*. The difference *P-L* is the upper limit of the
723     part of OXPHOS-capacity that is freely available for ATP production (corrected for LEAK-
724     respiration) and is fully coupled to phosphorylation with a maximum mechanistic stoichiometry
725     (**Fig. 7**).
726        **Control and regulation:** The terms metabolic *control* and *regulation* are frequently used
727     synonymously, but are distinguished in metabolic control analysis: 'We could understand the
728     regulation as the mechanism that occurs when a system maintains some variable constant over
729     time, in spite of fluctuations in external conditions (homeostasis of the internal state). On the
730     other hand, metabolic control is the power to change the state of the metabolism in response to
731     an external signal' (Fell 1997). Respiratory control may be induced by experimental control
732     signals that *exert* an influence on: (*1*) ATP demand and ADP phosphorylation-rate; (*2*) fuel
733     substrate composition, pathway competition; (*3*) available amounts of substrates and oxygen,
734     *e.g.*, starvation and hypoxia; (*3*) the protonmotive force, redox states, flux-force relationships,
735     coupling and efficiency; (*4*) $Ca^{2+}$ and other ions including $H^+$; (*5*) inhibitors, *e.g.*, nitric oxide
736     or intermediary metabolites, such as oxaloacetate; (*6*) signalling pathways and regulatory
737     proteins, *e.g.* insulin resistance, transcription factor HIF-1 or inhibitory factor 1. *Mechanisms*
738     of respiratory control and regulation include adjustments of: (*1*) enzyme activities by allosteric
739     mechanisms and phosphorylation; (*2*) enzyme content, concentrations of cofactors and
740     conserved moieties (such as adenylates, nicotinamide adenine dinucleotide [$NAD^+$/NADH],
741     coenzyme Q, cytochrome *c*); (*3*) metabolic channeling by supercomplexes; and *(4)*
742     mitochondrial density (enzyme concentrations and membrane area) and morphology (cristae
743     folding, fission and fusion). (*5*) Mitochondria are targeted directly by hormones, thereby
744     affecting their energy metabolism (Lee *et al.* 2013; Gerö and Szabo 2016; Price and Dai 2016;
745     Moreno *et al.* 2017). Evolutionary or acquired differences in the genetic and epigenetic basis
746     of mitochondrial function (or dysfunction) between subjects and gene therapy; age; gender,
747     biological sex, and hormone concentrations; life style including exercise and nutrition; and
748     environmental issues including thermal, atmospheric, toxicological and pharmacological

749 factors, exert an influence on all control mechanisms listed above. For reviews, see Brown
750 1992; Gnaiger 1993a, 2009; 2014; Paradies *et al.* 2014; Morrow *et al.* 2017.

751     **Respiratory control and response:** Lack of control by a metabolic pathway, *e.g.*
752 phosphorylation-pathway, does mean that there will be no response to a variable activating it,
753 *e.g.* [ADP]. However, the reverse is not true as the absence of a response to [ADP] does not
754 exclude the phosphorylation-pathway from having some degree of control. The degree of
755 control of a component of the OXPHOS-pathway on an output variable, such as oxygen flux,
756 will in general be different from the degree of control on other outputs, such as phosphorylation-
757 flux or proton leak flux. Therefore, it is necessary to be specific as to which input and output
758 are under consideration (Fell 1997).

759     **Respiratory coupling control:** Respiratory control refers to the ability of mitochondria
760 to adjust oxygen consumption in response to external control signals by engaging various
761 mechanisms of control and regulation. Respiratory control is monitored in a mitochondrial
762 preparation under conditions defined as respiratory states. When phosphorylation of ADP to
763 ATP is stimulated or depressed, an increase or decrease is observed in electron flux linked to
764 oxygen consumption in respiratory coupling states of intact mitochondria ('controlled states' in
765 the classical terminology of bioenergetics). Alternatively, coupling of electron transfer with
766 phosphorylation is disengaged by disruption of the integrity of the mtIM or by uncouplers,
767 functioning like a clutch in a mechanical system. The corresponding coupling control state is
768 characterized by high levels of oxygen consumption without control by phosphorylation
769 ('uncontrolled state').

770     **ET-pathway control states** are obtained in mitochondrial preparations by depletion of
771 endogenous substrates and addition to the mitochondrial respiration medium of fuel substrates
772 (CHNO; 2[H]) and specific inhibitors, activating selected mitochondrial catabolic pathways, k
773 (**Fig. 1 and 2**). Coupling control states and pathway control states are complementary, since
774 mitochondrial preparations depend on an exogenous supply of pathway-specific fuel substrates
775 and oxygen (Gnaiger 2014).

776

777 *2.3. Classical terminology for isolated mitochondria*
778     *'When a code is familiar enough, it ceases appearing like a code; one forgets that there*
779     *is a decoding mechanism. The message is identical with its meaning'* (Hofstadter 1979).

780

781 Chance and Williams (1955; 1956) introduced five classical states of mitochondrial respiration
782 and cytochrome redox states. **Table 3** shows a protocol with isolated mitochondria in a closed
783 respirometric chamber, defining a sequence of respiratory states. States and rates are not
784 specifically distinguished in this nomenclature.

785

786 **Table 3. Metabolic states of mitochondria (Chance and**
787 **Williams, 1956; Table V).**
788

| State | [$O_2$] | ADP level | Substrate Level | Respiration rate | Rate-limiting substance |
|-------|---------|-----------|-----------------|------------------|-------------------------|
| 1 | >0 | low | low | slow | ADP |
| 2 | >0 | high | ~0 | slow | substrate |
| 3 | >0 | high | high | fast | respiratory chain |
| 4 | >0 | low | high | slow | ADP |
| 5 | 0 | high | high | 0 | oxygen |

789

790     **State 1** is obtained after addition of isolated mitochondria to air-saturated
791 isoosmotic/isotonic respiration medium containing inorganic phosphate, but no fuel substrates
792 and no adenylates, *i.e.*, AMP, ADP, ATP.

**State 2** is induced by addition of a 'high' concentration of ADP (typically 100 to 300 µM), which stimulates respiration transiently on the basis of endogenous fuel substrates and phosphorylates only a small portion of the added ADP. State 2 is then obtained at a low respiratory activity limited by exhausted endogenous fuel substrate availability (**Table 3**). If addition of specific inhibitors of respiratory complexes, such as rotenone, does not cause a further decline of oxygen consumption, State 2 is equivalent to the state of residual oxygen consumption, ROX (See below.). If inhibition is observed, undefined endogenous fuel substrates are a confounding factor of pathway control, contributing to the effect of subsequently externally added substrates and inhibitors. In contrast to the original protocol, an alternative sequence of titration steps is frequently applied, in which the alternative 'State 2' has an entirely different meaning, when this second state is induced by addition of fuel substrate without ADP (LEAK-state; in contrast to State 2 defined in **Table 1** as a ROX state), followed by addition of ADP.

**State 3** is the state stimulated by addition of fuel substrates while the ADP concentration is still high (**Table 3**) and supports coupled energy transformation through oxidative phosphorylation. 'High ADP' is a concentration of ADP specifically selected to allow the measurement of State 3 to State 4 transitions of isolated mitochondria in a closed respirometric chamber. Repeated ADP titration re-establishes State 3 at 'high ADP'. Starting at oxygen concentrations near air-saturation (ca. 200 µM $O_2$ at sea level and 37 °C), the total ADP concentration added must be low enough (typically 100 to 300 µM) to allow phosphorylation to ATP at a coupled rate of oxygen consumption that does not lead to oxygen depletion during the transition to State 4. In contrast, kinetically-saturating ADP concentrations usually are an order of magnitude higher than 'high ADP', *e.g.* 2.5 mM in isolated mitochondria. The abbreviation State 3u is occasionally used in bioenergetics, to indicate the state of respiration after titration of an uncoupler, without sufficient emphasis on the fundamental difference between OXPHOS-capacity (*well-coupled* with an *endogenous* uncoupled component) and ET-capacity (*noncoupled*).

**State 4** is a LEAK-state that is obtained only if the mitochondrial preparation is intact and well-coupled. Depletion of ADP by phosphorylation to ATP leads to a decline in the rate of oxygen consumption in the transition from State 3 to State 4. Under these conditions of State 4, a maximum protonmotive force and high ATP/ADP ratio are maintained. For calculation of P»/$O_2$ ratios the gradual decline of $Y_{P»/O_2}$ towards diminishing [ADP] at State 4 must be taken into account (Gnaiger 2001). State 4 respiration, $L_T$ (**Table 1**), reflects intrinsic proton leak and intrinsic ATP hydrolysis activity. Oxygen consumption in State 4 is an overestimation of LEAK-respiration if the contaminating ATP hydrolysis activity recycles some ATP to ADP, $J_{P«}$, which stimulates respiration coupled to phosphorylation, $J_{P»} > 0$. This can be tested by inhibition of the phosphorylation-pathway using oligomycin, ensuring that $J_{P»} = 0$ (State 4o). Alternatively, sequential ADP titrations re-establish State 3, followed by State 3 to State 4 transitions while sufficient oxygen is available. However, anoxia may be reached before exhaustion of ADP (State 5).

**State 5** is the state after exhaustion of oxygen in a closed respirometric chamber. Diffusion of oxygen from the surroundings into the aqueous solution may be a confounding factor preventing complete anoxia (Gnaiger 2001). Chance and Williams (1955) provide an alternative definition of State 5, which gives it the different meaning of ROX versus anoxia: 'State 5 may be obtained by antimycin A treatment or by anaerobiosis'.

In **Table 3**, only States 3 and 4 (and 'State 2' in the alternative protocol: addition of fuel substrates without ADP without ADP; not included in the table) are coupling control states, with the restriction that $O_2$ flux in State 3 may be limited kinetically by non-saturating ADP concentrations (**Table 1**).

### 3. The protonmotive force, proton flux, and respiratory control

*3.1. Electric and chemical partial forces expressed in various units*

The protonmotive force across the mtIM, $\Delta p$ (Mitchell 1961; Mitchell and Moyle 1967), is a characteristic of respiratory states (**Table 1**). $\Delta p$ was introduced most elegantly in the *Grey Book 1966* (Mitchell 2011),

$$\Delta p = \Delta \Psi + \Delta \mu_{H+} \cdot F^{-1} \tag{2}$$

$\Delta p$ consists of two partial isomorphic forces: (*1*) The electric part, $\Delta \Psi$, is the electric potential difference§, which is not specific for $H^+$ and can, therefore, be measured by the distribution of any permeable cation equilibrating between the positive and negative compartment (**Fig. 2**). (*2*) The chemical part contains the chemical potential difference§ in $H^+$, $\Delta \mu_{H+}$, which is proportional to the pH difference, $\Delta pH$ (**Box 2**).

*Protonmotive* means that there is a potential for the movement of protons, and *force* is a measure of the potential for motion. Motion is relative and not absolute (Principle of Galilean Relativity); likewise there is no absolute potential, but isomorphic forces are stoichiometric potential *differences*§ related to $\Delta \Psi$ and $\Delta \mu_{H+}$ (**Table 4**). $F$ is the Faraday constant (**Table 5**). According to its definition in physics, a potential difference and as such the *protonmotive force* is not a force *per se* (IUPAC: Cohen *et al.* 2008). Forces as defined in physics, $\boldsymbol{F}$ [N ≡ J·m$^{-1}$ = m·kg·s$^{-2}$], describe the interaction between particles as vectors with direction of a gradient in space. These forces cause a change in the motion (acceleration) of the particles in the spatial direction of the force. The fundamental forces are the gravitational, electroweak (combining electromagnetic and weak nuclear) and strong nuclear forces. In contrast to the *gradient-forces with spatial direction*, the compartmental forces are stoichiometric potential differences, distinguished as isomorphic *motive delta-forces*, $\Delta_{tr}F$, *with compartmental direction* of the energy transformation, tr (**Box 3**). The delta-forces are expressed in various *motive units*, MU [J·MU$^{-1}$], depending on the energy transformation under study and on the unit chosen to express the motive entity and advancement of the process. For the protonmotive force the proton is the *motive entity*, which can be expressed in a variety of formats with different MU. Consistency of terms and symbols can be achieved with reference to motive delta-forces, $\Delta_{tr}F$, which express explicitly the meaning of the terms in Eq.(2) and show their connection (**Table 4**).

The electric and chemical components of the protonmotive force are added (motive = electric + chemical; Eq. 2). Since a physical quantity is the product of a numerical value and a unit, such addition is possible only when the partial forces are expressed in a common format with identical units (**Box 2**). Among the ultimate unifying principles in physics is the concept of the particle. The protonmotive force can be expressed per particle (per proton), in which case the MU for the proton is a pure number [x], and the unit of the *molecular force* is [J·x$^{-1}$]. When the number of particles or molecules, $N$ [x], is divided by the Avogadro constant, $N_A$ [x·mol$^{-1}$], the *molecular motive unit* [x] is converted to the *molar motive unit* mole [mol], whereas multiplication of $N$ by $e$ [C·x$^{-1}$] yields the *electrical motive unit* coulomb [C] (**Fig. 8**). When the protonmotive force is expressed in the electrical MU-format as a voltage (electrochemical stoichiometric potential difference§; Eq. 2), the MU is the coulomb, and the unit of the *electrical force* is [J·C$^{-1}$ ≡ V]. The molar MU-format of Eq.(2) is known as the chemiosmotic potential difference§, where the MU is the mole, and the unit of the *molar force* is [J·mol$^{-1}$].

The protonmotive force, $\Delta_m F_{H+}$ [J·MU$^{-1}$], is conjugated to the transmembrane proton flux, $J_{mH+}$ [MU·s$^{-1}$·m$^{-3}$]. Conjugated quantities are linked by the same MU; in other words, they are expressed in the same MU-format. When different MU-formats are used, the format ($N$, $\boldsymbol{n}$, $e$) is shown as a subscript (**Fig. 8**). Further formats are theoretically possible, *e.g.*, mass (MU=kg), or energy with further specification (MU=J).

**Table 4. Protonmotive force and flux matrix.** Rows: Compartmental proton flux (rate) and protonmotive force (state). Molecular, molar and electrical formats (*N*, *n* and *e*) with motive units, MU, of particle number, $N$ [x], amount of substance, $n$ [mol] and electric charge [C], respectively. Columns: The protonmotive force, $\Delta_m F_{H+}$, is the sum of two *partial isomorphic forces*, $\Delta_{el}F_{H+} + \Delta_d F_{H+}$. In contrast to force, the conjugated flux cannot be partitioned but is expressed in different MU-formats.

| State | Name | | motive m | = | electric el | + | chemical d | Unit | Notes |
|---|---|---|---|---|---|---|---|---|---|
| **Rate** | **isomorphic flux** | | $J_{mH+}$ | | | | | MU·s$^{-1}$·m$^{-3}$ | 1 |
| | *N* | molecular | $J_{mH+N}$ | | | | | x·s$^{-1}$·m$^{-3}$ | 1*N* |
| | *n* | molar | $J_{mH+n}$ | | | | | mol·s$^{-1}$·m$^{-3}$ | 1*n* |
| | *e* | electrical | $J_{mH+e}$ | | | | | C·s$^{-1}$·m$^{-3}$ | 1*e* |
| **State** | **isomorphic force** | | $\Delta_m F_{H+}$ | = | $\Delta_{el}F_{H+}$ | + | $\Delta_d F_{H+}$ | J·MU$^{-1}$ | 2 |
| | *N* | molecular | $\Delta_m F_{H+N}$ | = | $\Delta_{el}F_{H+N}$ | + | $\Delta_d F_{H+N}$ | J·x$^{-1}$ | 2*N* |
| | *n* | molar | $\Delta_m F_{H+n}$ | = | $\Delta_{el}F_{H+n}$ | + | $\Delta_d F_{H+n}$ | J·mol$^{-1}$ | 2*n* |
| | *e* | electrical | $\Delta_m F_{H+e}$ | = | $\Delta_{el}F_{H+e}$ | + | $\Delta_d F_{H+e}$ | J·C$^{-1}$ | 2*e* |
| | *n* | chemiosmotic potential | $\Delta\widetilde{\mu}_{H+}$ | = | $\Delta\Psi \cdot z_{H+}\cdot F$ | + | $\Delta\mu_{H+}$ | J·mol$^{-1}$ | 3*n*§ |
| | *e* | protonmotive force | $\Delta p$ | = | $\Delta\Psi \cdot z_{H+}$ | + | $\Delta\mu_{H+}\cdot F^{-1}$ | J·C$^{-1}$ | 3*e*§ |

1: The sign of the flux, $J_{mH+}$, depends on the definition of the compartmental direction of the translocation. Flux in the outward direction into the positively (pos) charged compartment, $J_{mH+pos}$, is positive when $H^+_{pos}$ is added to the pos-compartment ($v_{H+pos} = 1$), and $H^+_{neg}$ is removed stoichiometrically ($v_{H+neg} = -1$). Conversely, $J_{mH+neg}$ is positive when $H^+_{neg}$ is added to the negatively charged compartment ($v_{H+neg} = 1$) and $H^+_{pos}$ is removed ($v_{H+pos} = -1$; **Fig. 2**).

2: $\Delta_m F_{H+}$ is the protonmotive force per entity $H^+$ (not per e$^-$) expressed in any MU-format. $\Delta_{el}F_{H+}$ is the partial protonmotive force (el) acting generally on charged motive elements (*i.e.*, ions that are permeable across the mtIM). In contrast, $\Delta_d F_{H+}$ is the partial protonmotive force specific for proton diffusion (d) irrespective of charge. The sign of the force is negative for exergonic transformations in which exergy is lost or dissipated, $\Delta_m F_{H+neg}$, and positive for endergonic transformations which conserve exergy in a coupled exergonic process, $\Delta_m F_{H+pos} = -\Delta_m F_{H+neg}$ (**Box 3**). By definition, the product of flux and force is volume-specific power [J·s$^{-1}$·m$^{-3}$ = W·m$^{-3}$]: $P_{V,mH+} = J_{mH+pos_e}\cdot\Delta_m F_{H+pos_e} = J_{mH+pos_n}\cdot\Delta_m F_{H+pos_n}$.

3: 3*n* and 3*e* are the classical representations of 2*n* ($\Delta_d F_{H+n} \equiv \Delta\mu_{H+}$)§ and 2*e* ($\Delta_{el}F_{H+e} \equiv \Delta\Psi\cdot z$)§; $z = z_{H+}$. For further details see **Box 2**.



$N$ to *n*: $J_{mH+N}\cdot N_A^{-1}$ $= J_{mH+n}$ [mol·s$^{-1}$·m$^{-3}$]   $\Delta_m F_{H+N}\cdot N_A$ $= \Delta_m F_{H+n}$ [J·mol$^{-1}$]

$N$ to *e*: $J_{mH+N}\cdot e$ $= J_{mH+e}$ [C·s$^{-1}$·m$^{-3}$]   $\Delta_m F_{H+N}\cdot e^{-1}$ $= \Delta_m F_{H+e}$ [J·C$^{-1}$]

*n* to *e*: $J_{mH+n}\cdot(e\cdot N_A)$ $= J_{mH+e}$ [C·s$^{-1}$·m$^{-3}$]   $\Delta_m F_{H+n}\cdot(e\cdot N_A)^{-1}$ $= \Delta_m F_{H+e}$ [J·C$^{-1}$]
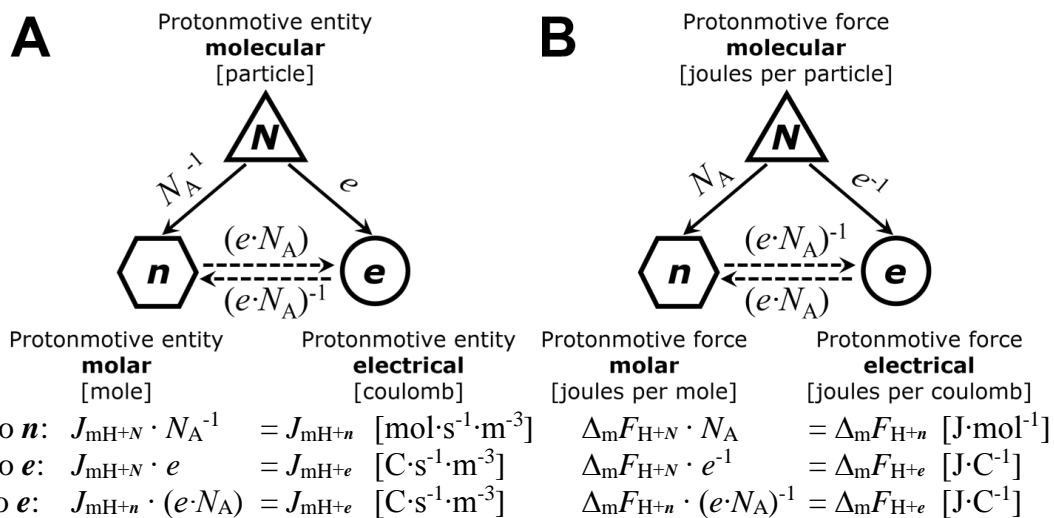
**Fig. 8. Molecular, molar and electrical (*N, n, e*) formats and units of the protonmotive entity (A) and protonmotive force (B).** Avogadro constant, $N_A$: H$^+$ per mol H$^+$ [x·mol$^{-1}$]; elementary charge, $e$: coulombs per electron [C·x$^{-1}$] (**Table 5**).

927      Unfortunately, the dimensionless unit [x] is not explicitly considered by IUPAC (Mohr
928 and Philipps 2015). This causes confusion, since then the unit [J] (per system or per particle)
929 would indicate either an extensive quantity (energy per system [J]) or intensive quantity (force,
930 energy per motive particle [J·x$^{-1}$]) (**Box 2**). Even though the charge number $z$ equals 1 for the
931 proton, $z$ should be written explicitly in Eq.(2) for physical consistency. $z$ is not involved in the
932 conversion of motive units (**Fig. 8**), in contrast to a change not only of units but transition from
933 the *entity of the proton to the entity of charge* ($zF = ze \cdot N_A$; **Table 5**): The ratio of electrons per
934 proton ($z_{H+}=1$) is multiplied by the elementary charge ($e$, coulombs per electron), which yields
935 coulombs per proton [C·x$^{-1}$]. This is multiplied with $N_A$ (protons per mole protons [x·mol$^{-1}$]),
936 thus obtaining for $ze \cdot N_A$ the ratio of *coulombs charge* per *mole protons* [C·mol$^{-1}$].
937

---

938 **Box 2: The partial protonmotive forces and conversion between motive units**
939
940 The separation of partial isomorphic (electric and chemical) forces as the components of the
941 protonmotive force (**Table 4**) must be clearly distinguished from expressing $\Delta_m F_{H+}$ in different
942 motive units (MU) or MU-formats.
943
944     **Protonmotive force, three MU-formats** (**Fig. 8B**)
945     $N$ molecular format:  $\Delta_m F_{H+N}$       $= \Delta_m F_{H+n} \cdot N_A^{-1}$  $= \Delta_m F_{H+e} \cdot e$       [J·x$^{-1}$]
946     $n$  molar format:      $\Delta_m F_{H+n} \equiv \Delta \tilde{\mu}_{H+}$  $= \Delta_m F_{H+N} \cdot N_A$  $= \Delta_m F_{H+e} \cdot (e \cdot N_A)$  [J·mol$^{-1}$]
947     $e$  electrical format:  $\Delta_m F_{H+e} \equiv \Delta p$   $= \Delta_m F_{H+N} \cdot e^{-1}$  $= \Delta_m F_{H+n} \cdot (e \cdot N_A)^{-1}$ [J·C$^{-1}$] $\equiv$ [V]
948
949 Irrespective of format, the proton is the current-carrying entity (Kell 1979). Conversion
950 between MU-formats is based on fundamental physical constants (**Table 5**). The Faraday
951 constant, $F = e \cdot N_A$ [C·mol$^{-1}$], is the product of elementary charge per particle, $e$ [C·x$^{-1}$], and the
952 Avogadro (Loschmidt) constant, $N_A$ [x·mol$^{-1}$]. Taken together, $e \cdot N_A$ is the conversion factor
953 between electrical and chemical units. $\Delta_m F_{H+e}$ [J·C$^{-1}$] is expressed per motive protons in units
954 *charge* [C], whereas $\Delta_m F_{H+n} = \Delta_m F_{H+e} \cdot (e \cdot N_A)$ [J·mol$^{-1}$] is expressed per motive protons in units
955 *amount* [mol] (**Fig. 8**).
956
957 **el:**   **Electric part of the protonmotive force, three MU-formats**
958     $N$  $\Delta_{el} F_{H+N}$, partial electric Gibbs energy change per *motive proton*, $N_{H+}$ [J·x$^{-1}$].
959     $n$  $\Delta_{el} F_{H+n} = \Delta \Psi \cdot zF$;[§] electric force expressed in chemical units joule per mole protons
960        [J·mol$^{-1}$], defined as partial electric Gibbs energy change per *motive protons expressed as
961        amount in units mole*, $n_{H+}$ [mol], not specific for proton charge.
962     $e$  $\Delta_{el} F_{H+e} \equiv \Delta \Psi \cdot z$;[§] electric part of the protonmotive force expressed in electrical units joule
963        per coulomb protons, *i.e.*, volt [J·C$^{-1}$ $\equiv$ V], defined as partial electric Gibbs energy change
964        per *motive protons expressed in units coulomb* [C], not specific for proton charge.
965
966 **d:**   **Chemical part (diffusion, d) of the protonmotive force, three MU-formats**
967     $N$  $\Delta_d F_{H+N}$, partial Gibbs energy change per *motive proton*, $N_{H+}$ [J·x$^{-1}$].
968     $n$  $\Delta_d F_{H+n} \equiv \Delta \mu_{H+}$;[§] chemical part (diffusion, translocation) of the protonmotive force
969        expressed in units joule per mole [J·mol$^{-1}$], defined as partial Gibbs energy change per
970        *motive amount of protons, $n_{H+}$* [mol].
971     $e$  $\Delta_d F_{H+e} = \Delta \mu_{H+} \cdot F^{-1}$;[§] chemical force expressed in units joule per coulomb of protons
972        [J·C$^{-1}$], defined as partial Gibbs energy change per *motive amount of protons expressed
973        in units coulomb* [C], specific for the proton as the motive entity.
974
975 Consider B$^z$ as a cation that is permeable across the mtIM and is in equilibrium between the
976 positive and negative compartments. The ionmotive force, $\Delta_m F_{Bz}$, is zero at equilibrium, when
977 the electric and chemical partial forces compensate each other (compare Eq. 2 in **Table 4**):
978
979

General: $\Delta_m F_{Bz} = \Delta_{el} F_{Bz} + \Delta_d F_{Bz}$

At equilibrium: $\Delta_m F_{Bz} = 0$     $0 = \Delta_{el} F_{Bz} + \Delta_d F_{Bz}$     $\Delta_{el} F_{Bz} = -\Delta_d F_{Bz}$

For distribution of cation $B^z$ between the negative and positive compartment (**Fig. 2**), an equilibrium concentration ratio (strictly activity ratio; **Table 6**) is obtained, $c_{Bzneg}/c_{Bzpos}$, the natural logarithm of which is $\Delta \ln c_{Bz} = \ln(c_{Bzneg}/c_{Bzpos})$. Multiplication of $\Delta \ln c_{Bz}$ by $RT$ [J·mol$^{-1}$] or $kT$ [J·x$^{-1}$] yields the partial chemical force, $\Delta_d F_{Bz}$, as exergy per mole (format **n**, based on the gas constant) or exergy per particle (format **N**, based on the Boltzmann constant; **Table 5**). The MU-formats are interconverted as follows, considering *equilibrium* as described above:[§]

**N**:  $\Delta_{el} F_{Bz,N} = \Delta\psi \cdot ze = -\Delta_d F_{Bz,N} = -RT \cdot N_A^{-1} \cdot \Delta\ln c_{Bz} = -kT \cdot \Delta\ln c_{Bz}$

**n**:  $\Delta_{el} F_{Bz,n} = \Delta\psi \cdot ze \cdot N_A = -\Delta_d F_{Bz,n} = -RT \cdot \Delta\ln c_{Bz} = -kT \cdot N_A \cdot \Delta\ln c_{Bz}$

**e**:  $\Delta_{el} F_{Bz,e} \equiv \Delta\psi \cdot z = -\Delta_d F_{Bz,e} = -RT \cdot (e \cdot N_A)^{-1} \cdot \Delta\ln c_{Bz} = -kT \cdot e^{-1} \cdot \Delta\ln c_{Bz}$

In the special case of zero $\Delta$pH, $\Delta_m F_{H+} = \Delta_{el} F_{H+}$ ($\Delta p = \Delta\psi$;[§] Eq. 2).

Due to the low permeability of the mtIM for protons and the action of the respiratory proton pumps, there is no equilibration of protons between the positive and negative compartments. Therefore, the protonmotive force, $\Delta_m F_{H+}$, is not zero, and $\Delta_{el} F_{H+}$ cannot be calculated from the proton distribution as described for the equilibrating cation $B^z$ above. With $\Delta \ln c_{H+} = -\ln(10) \cdot \Delta$pH $= -2.3 \cdot \Delta$pH, the MU-formats for the chemical part of the protonmotive force are interconverted as described above:[§]

**N**:  $\Delta_d F_{H+N} = \Delta\mu_{H+} \cdot N_A^{-1} = RT \cdot N_A^{-1} \cdot \Delta\ln c_{H+} = kT \cdot \Delta\ln c_{H+}$

**n**:  $\Delta_d F_{H+n} \equiv \Delta\mu_{H+} = RT \cdot \Delta\ln c_{H+} = kT \cdot N_A \cdot \Delta\ln c_{H+}$

**e**:  $\Delta_d F_{H+e} = \Delta\mu_{H+} \cdot (e \cdot N_A)^{-1} = RT \cdot (e \cdot N_A)^{-1} \cdot \Delta\ln c_{H+} = kT \cdot e^{-1} \cdot \Delta\ln c_{H+}$

**Table 5: Fundamental physical MU-formats, constants, and relationships**

| Format | Name | Abbreviation | Value (Gibney et al 2017)* | Unit |
|---|---|---|---|---|
| **N** | molecular, particle | | | MU = x |
| **n** | molar, chemical | | | MU = mol |
| **e** | electrical | | | MU = C |
| **N** | Boltzmann constant* | $k$ | $k = 1.380649 \cdot 10^{-23}$ | J·x$^{-1}$ ·K$^{-1}$ |
| **n** | Gas constant | $R = k \cdot N_A$ | $k \cdot N_A = 8.31451$ | J·mol$^{-1}$·K$^{-1}$ |
| **e** | $R \cdot F^{-1} = k \cdot e^{-1}$ (*no name*) | $R \cdot F^{-1} = k \cdot e^{-1}$ | $k \cdot e^{-1} = 8.617333 \cdot 10^{-5}$ | J·C$^{-1}$ ·K$^{-1}$ |
| **N/n** | Avogadro constant* | $N_A = N/n$ | $N_A = 6.02214076 \cdot 10^{23}$ | x·mol$^{-1}$ |
| **e/N** | elementary charge* | $e$ | $e = 1.602176634 \cdot 10^{-19}$ | C·x$^{-1}$ |
| **e/n** | Faraday constant | $F = e \cdot N_A$ | $e \cdot N_A = 96{,}485.33$ | C·mol$^{-1}$ |

The electric partial force is indicated by subscript 'el': $\Delta_{el} F_{H+}$. Correspondingly, the chemical partial force of diffusion is indicated by subscript 'd': $\Delta_d F_{H+}$, with focus on the particle separate from the charge (**Table 4**). The total motive force (motive = electric + chemical) is distinguished from the partial components by subscript 'm', $\Delta_m F_{H+}$. Reading this symbol by starting with the proton, it can be seen as pmf, or the subscript m (motive) can be remembered by the name of Mitchell.

1033    The compartmental direction of movement *into the positive compartment* is shown by
1034 subscript 'pos' for the force and flux: $\Delta_m F_{H+pos}$ and $J_{mH+pos}$ (**Fig. 2**). The sign of the force is
1035 positive, when Gibbs energy is conserved in proton pumping. When the direction of flux is
1036 defined as movement into the negative compartment, $J_{mH+neg}$, the force, $\Delta_m F_{H+neg}$, has a negative
1037 sign in the dissipative direction (**Box 4**).
1038    A partial electric force of 0.2 V in the electrical format, $\Delta_{el} F_{H+pos,e}$ (**Table 6**, Note 5**e**), is
1039 19 kJ·mol$^{-1}$ H$^+_{pos}$ in the molar format, $\Delta_{el} F_{H+pos,n}$ (Note 5**n**). For 1 unit of $\Delta pH$, the partial
1040 chemical force changes by -5.9 kJ·mol$^{-1}$ in the molar format, $\Delta_d F_{H+pos,n}$ (**Table 6**, Note 6**n**), and
1041 by -0.06 V in the electrical format, $\Delta_d F_{H+pos,e}$ (Note 6**e**). Considering a driving force of -470
1042 kJ·mol$^{-1}$ O$_2$ for oxidation, the thermodynamic limit of the H$^+_{pos}$/O$_2$ ratio is reached at a value of
1043 470/19 = 24, compared to a mechanistic stoichiometry of 20 (**Fig. 1**).
1044
1045
1046 ## Table 6. Power, exergy, force, flux, and advancement.

| Expression | Symbol | Definition | Unit | Notes |
|---|---|---|---|---|
| power, volume-specific | $P_{V,tr}$ | $P_{V,tr} = J_{tr} \cdot \Delta_{tr}F = d_{tr}G \cdot dt^{-1} \cdot V^{-1}$ | J·s$^{-1}$·m$^{-3}$ | 1 |
| force, compartmental | $\Delta_{tr}F$ | $\Delta_{tr}F = \partial G \cdot \partial_{tr}\xi^{-1}$ | J·MU$^{-1}$ | 2 |
| flux, compartmental | $J_{tr}$ | $J_{tr} = d_{tr}\xi \cdot dt^{-1} \cdot V^{-1}$ | MU·s$^{-1}$·m$^{-3}$ | 3 |
| advancement, **n** | $d_{tr}\xi_{H+n}$ | $d_{tr}\xi_{H+n} = d_{tr}n_{H+} \cdot v_{H+}^{-1}$ | MU=mol | 4**n** |
| advancement, **e** | $d_{tr}\xi_{H+e}$ | $d_{tr}\xi_{H+e} = d_{tr}e_{H+} \cdot v_{H+}^{-1}$ | MU=C | 4**e** |
| electric partial force, **n** | $\Delta_{el}F_{Bz,n}$ | $\Delta_{el}F_{Bz,n} = -RT \cdot \Delta \ln c_{Bz}$ $= 96.5 \cdot \Delta\Psi \cdot z$ | J·mol$^{-1}$ kJ·mol$^{-1}$ | 5**n** § |
| electric partial force, **e** | $\Delta_{el}F_{Bz,e}$ | $\Delta_{el}F_{Bz,e} = -RT/F \cdot \Delta \ln c_{Bz}$ | V = J·C$^{-1}$ | 5**e** |
| chemical partial force, **n** at 37 °C | $\Delta_d F_{H+n}$ | $\Delta_d F_{H+n} = -RT \cdot \ln(10) \cdot \Delta pH$ $= -5.9 \cdot \Delta pH$ | J·mol$^{-1}$ kJ·mol$^{-1}$ | 6**n** |
| chemical partial force, **e** at 37 °C | $\Delta_d F_{H+e}$ | $\Delta_d F_{H+e} = -RT/F \cdot \ln(10) \cdot \Delta pH$ $= -0.061 \cdot \Delta pH$ | J·C$^{-1}$ J·C$^{-1}$ | 6**e** |

1047
1048 1 to 4:  The *SI* unit of power is watt [W ≡ J·s$^{-1}$]. A motive entity, expressed in a motive unit [MU] is a
1049 characteristic for any type of transformation, tr.
1050 2:    Isomorphic forces, $\Delta_{tr}F$, are related to the generalized forces, $X_{tr}$, of irreversible thermodynamics
1051 as  $\Delta_{tr}F = -X_{tr} \cdot T$, and the force of chemical reactions is the negative affinity, $\Delta_r F = -A$ (Prigogine
1052 1967). $\partial G$ [J] is the partial Gibbs energy (exergy) change in the advancement of transformation
1053 tr.
1054 3:    For MU = C, flow is electric current, $I_{el}$ [A ≡ C·s$^{-1}$], flux is electric current density per area, $J_{el}$, and
1055 compartmental flux is electric current density per volume, $I_{el}$ [A·m$^{-3}$], all expressed in electrical
1056 format.
1057 4:    For a chemical reaction, the advancement of reaction r is $d_r\xi_B = d_r n_B \cdot v_B^{-1}$ [mol]. The stoichiometric
1058 number is $v_B = -1$ or $v_B = 1$, depending on B being a product or substrate, respectively, in reaction
1059 r involving one mole of B. The conjugated *intensive* molar quantity, $\Delta_r F_B = \partial G / \partial_r \xi_B$ [J·mol$^{-1}$], is the
1060 chemical force of reaction or *reaction-motive* force per stoichiometric amount of B. In reaction
1061 kinetics, $d_r n_B$ is expressed as a volume-specific quantity, which is the partial contribution to the
1062 total concentration change of B, $d_r c_B = d_r n_B / V$ and $dc_B = dn_B / V$, respectively. In open systems with
1063 constant volume V, $dc_B = d_r c_B + d_e c_B$, where r indicates the *internal* reaction and e indicates the
1064 *external* flux of B into the unit volume of the system. At steady state the concentration does not
1065 change, $dc_B = 0$, when $d_r c_B$ is compensated for by the external flux of B, $d_r c_B = -d_e c_B$ (Gnaiger
1066 1993b). Alternatively, $dc_B = 0$ when B is held constant by different coupled reactions in which B
1067 acts as a substrate or a product.

5:   Stoichiometric potential difference[§] across the mtIM. In a scalar electric transformation (flux of charge, *i.e.*, volume-specific current, from the matrix space to the intermembrane and extramitochondrial space), the motive force is the stoichiometric difference of charge (**Box 2**). The endergonic direction of translocation is defined in **Fig. 2** as $H^+_{neg} \rightarrow H^+_{pos}$. $F = 96.5$ (kJ·mol$^{-1}$)/V (**Table 5**). $z$ is the charge number of ion B. $a_B$ is the (relative) activity of ion B, which in dilute solutions ($c < 0.1$ mol·dm$^{-3}$) is approximately equal to $c_B/c°$, where $c°$ is the standard concentration of 1 mol·dm$^{-3}$. Note that ion selective electrodes (pH or TPP$^+$ electrodes) respond to ln $a_B$. $\Delta$ln $a_{H+}$ = $-\ln(10)\cdot\Delta$pH (**Box 2**).

6:   $RT$ = 2.479 and 2.579 kJ·mol$^{-1}$ at 298.15 and 310.15 K (25 and 37 °C), respectively (**Table 5**).

6*n*:   $\ln(10)\cdot RT$ = 5.708 and 5.938 kJ·mol$^{-1}$ at 298.15 and 310.15 K, respectively. Replacing the gas constant, $R$, by the Boltzmann constant, $k$, converts the molar format, *n* [J·mol$^{-1}$] into the molecular format, *N* [J·x$^{-1}$] (**Box 2**).

6*e*:   $RT/(zF)$ = 2.479 and 2.579 mV at 298.15 and 310.15 K, respectively, and $\ln(10)\cdot RT/(zF)$ = 59.16 and 61.54 mV, respectively, for $z = 1$.

**Vectorial and scalar forces, and fluxes:** We place the concept of the protonmotive force into the general context of physical chemistry. Complementary to the attempt towards unification of fundamental forces defined in physics, the concepts of Nobel laureates Lars Onsager, Erwin Schrödinger, Ilya Prigogine and Peter Mitchell unite (even if expressed in apparently unrelated terms) the diversity of *generalized* or 'isomorphic' *flux-force* relationships, the product of which links to entropy production and the Second Law of thermodynamics (Schrödinger 1944; Prigogine 1967). A *motive force* is the derivative of potentially available or 'free' energy (exergy) per advancement of a *motive elementary entity* (**Box 3**). Perhaps the first account of a *motive force* in energy transformation can be traced back to the Peripatetic school around 300 BC in the context of moving a lever, up to Newton's motive force proportional to the alteration of motion (Coopersmith 2010). As a generalization, isomorphic motive forces are considered as *entropic forces* in physics (Wang 2010).

The forces of vectoral diffusion and scalar chemical reactions are isomorphic. Both types of transformation do not have spatial but compartmental direction. The compartments are separated energetically as the initial and final compartments (*e.g.*, outer and inner) for diffusion (pos and neg; **Fig. 2**) or as the substrate and product compartments for chemical reactions. The corresponding vectorial and scalar fluxes (**Box 3**) are expressed per volume of the system (**Fig. 2**). The conjugated motive forces are *differences* between compartments (**Table 6**), without taking into account the *gradients* across the 6 nm thick mtIM.

---

**Box 3: Metabolic fluxes and flows: vectorial and scalar**

In mitochondrial electron transfer (**Fig. 1**), vectorial transmembrane proton flux is coupled through the proton pumps CI, CIII and CIV to the catabolic flux of scalar reactions, collectively measured as oxygen flux. In **Fig. 2**, the scalar catabolic reaction, k, of oxygen consumption, $J_{kO_2}$ [mol·s$^{-1}$·m$^{-3}$], is expressed as oxygen flux per volume, $V$ [m$^3$], of the instrumental chamber (the system).

Fluxes are *vectors*, if they have *spatial* geometric direction in addition to magnitude. Electric charge per unit time is electric flow or current, $I_{el} = dQ_{el}\cdot dt^{-1}$ [A]. When expressed per unit cross-sectional area, $A$ [m$^2$], a vector flux is obtained, which is current density or surface-density of flow) perpendicular to the direction of flux, $J_{el} = I_{el}\cdot A^{-1}$ [A·m$^{-2}$] (Cohen et al. 2008). For all transformations *flows*, $I_{tr}$, are defined as extensive quantities. Vector and scalar *fluxes* are obtained as $J_{tr} = I_{tr}\cdot A^{-1}$ [mol·s$^{-1}$·m$^{-2}$] and $J_{tr} = I_{tr}\cdot V^{-1}$ [mol·s$^{-1}$·m$^{-3}$], expressing flux as an area-specific vector or volume-specific vectorial or scalar quantity, respectively (Gnaiger 1993b).

We suggest to define: (*1*) *vectoral* fluxes, which are translocations as functions of *gradients* with direction in geometric space in continuous systems; (*2*) *vectorial* fluxes, which describe translocations in discontinuous systems and are restricted to information on *compartmental differences* (**Fig. 2**, transmembrane proton flux); and (*3*) *scalar* fluxes, which are transformations in a *homogenous* system (**Fig. 2**, catabolic $O_2$ flux, $J_{kO_2}$).

1122       Vectorial transmembrane proton fluxes, $J_{mH+pos}$ and $J_{mH+neg}$, are analyzed in a
1123  heterogenous compartmental system as a quantity with *directional* but not *spatial* information.
1124  Translocation of protons across the mtIM has a defined direction, either from the negative
1125  compartment (matrix space; negative, neg-compartment) to the positive compartment (inter-
1126  membrane space; positive, pos-compartment) or *vice versa* (**Fig. 2**). The arrows defining the
1127  direction of the translocation between the two compartments may point upwards or downwards,
1128  right or left, without any implication that these are actual directions in space. The pos-
1129  compartment is neither above nor below the neg-compartment in a spatial sense, but can be
1130  visualized arbitrarily in a figure in the upper position (**Fig. 2**). In general, the *compartmental*
1131  *direction* of vectorial translocation from the neg-compartment to the pos-compartment is
1132  defined by assigning the initial and final state as *ergodynamic compartments*, $H^+_{neg} \rightarrow H^+_{pos}$ or
1133  $0 = -1\ H^+_{neg} + 1\ H^+_{pos}$, related to work (erg = work; **Box 4**) that must be performed to lift the
1134  proton from a lower to a higher electrochemical potential or from the lower to the higher
1135  ergodynamic compartment (Gnaiger 1993b).
1136       In analogy to *vectorial* translocation, the direction of a *scalar* chemical reaction, $A \rightarrow B$
1137  or $0 = -1\ A + 1\ B$, is defined by assigning substrates and products, A and B, as ergodynamic
1138  compartments. $O_2$ is defined as a substrate in respiratory $O_2$ consumption, which together with
1139  the fuel substrates comprises the substrate compartment of the catabolic reaction (**Fig. 2**).
1140  Volume-specific scalar $O_2$ flux is coupled (**Box 5**) to vectorial translocation. In order to
1141  establish a quantitative relation between the coupled fluxes, both $J_{kO_2}$ and $J_{mH+pos}$ must be
1142  expressed in identical units, $[mol \cdot s^{-1} \cdot m^{-3}]$ or $[C \cdot s^{-1} \cdot m^{-3}]$, yielding the $H^+_{pos}/O_2$ ratio (**Fig. 1**). The
1143  *vectorial* proton flux in compartmental translocation has *compartmental direction*,
1144  distinguished from a *vector* flux with *spatial direction*. Likewise, the corresponding
1145  protonmotive force is linked to electrochemical potential *differences*[§] between two
1146  compartments, in contrast to a *gradient* across the membrane or a vector force with defined
1147  spatial direction.

1148
1149  *3.2. Coupling and efficiency*
1150
1151     **Coupling:** In energetics (ergodynamics), coupling is defined as an energy transformation
1152  fuelled by an exergonic (downhill) input process driving the advancement of an endergonic
1153  (uphill) output process (**Box 4**). The (negative) output/input power ratio is the efficiency of a
1154  coupled energy transformation (**Box 5**). At the limit of maximum efficiency of a completely
1155  coupled system, the (negative) input power equals the (positive) output power, such that the
1156  total power approaches zero at the maximum efficiency of 1, and the process becomes fully
1157  reversible without any dissipation of exergy, *i.e.*, without entropy production.

1158

---

1159  **Box 4: Endergonic and exergonic transformations, exergy and dissipation**
1160
1161  A chemical reaction, and any transformation, is exergonic if the Gibbs energy change (exergy)
1162  of the reaction is negative at constant temperature and pressure. The sum of Gibbs energy
1163  changes of all internal transformations in a system can only be negative, *i.e.*, exergy is
1164  irreversibly dissipated. Endergonic reactions are characterized by positive Gibbs energies of
1165  reaction and cannot proceed spontaneously in the forward direction as defined. For instance,
1166  the endergonic reaction P» is coupled to exergonic catabolic reactions, such that the total Gibbs
1167  energy change is negative, *i.e.*, exergy must be dissipated for the reaction to proceed (**Fig. 2**).
1168     In contrast, energy cannot be lost or produced in any internal process, which is the key
1169  message of the First Law of thermodynamics. Thus mitochondria are the sites of energy
1170  transformation but not energy production. Open and closed systems can gain energy and exergy
1171  only by external fluxes, *i.e.*, uptake from the environment. Exergy is the potential to perform
1172  work. In the framework of flux-force relationships (**Box 5**), the *partial* derivative of Gibbs

energy per advancement of a transformation is an isomorphic force, $\Delta_{tr}F$ (**Table 6**, Note 2). In other words, force is equal to exergy per advancement of a motive entity (in integral form, this definition takes care of non-isothermal processes). This formal generalization represents an appreciation of the conceptual beauty of Peter Mitchell's innovation of the protonmotive force against the background of the established paradigm of the electromotive force (emf) defined at the limit of zero current (Cohen *et al.* 2008).

---

**Box 5: Coupling, power and efficiency, at constant temperature and pressure**

Energetic coupling means that two processes of energy transformation are linked such that the input power, $P_{in}$, is the driving element of the output power, $P_{out}$, and the (negative) out/input power ratio is the efficiency. In general, power is work per unit time [J·s$^{-1}$ ≡ W]. When describing a system with volume $V$ without information on the internal structure, the output is defined as the *external* work performed by the *total* system on its environment. Such a system may be open for any type of exchange, or closed and thus allowing only heat and work to be exchanged across the system boundaries. This is the classical black box approach of thermodynamics. In contrast, in a colourful compartmental analysis of *internal* energy transformations (**Fig. 2**), the system is structured and described by definition of ergodynamic compartments (with information on the heterogeneity of the system; **Box 3**) and analysis of separate parts, *i.e.*, a sequence of *partial* energy transformations, tr. At constant temperature and pressure, power per unit volume, $P_{V,tr} \equiv P_{tr}/V$ [W·m$^{-3}$], is the product of a volume-specific flux, $J_{tr}$, and its conjugated force, $\Delta_{tr}F$, and is directly linked to entropy production, $d_iS/dt = \Sigma_{tr}P_{tr}/T$ [W·K$^{-1}$], as generalized by irreversible thermodynamics (Prigogine 1967; Gnaiger 1993a,b). Output power of proton translocation and catabolic input power are (**Fig. 2**),

$$\text{Output:} \qquad P_{mH+pos}/V = J_{mH+pos} \cdot \Delta_m F_{H+pos}$$
$$\text{Input:} \qquad P_{kO_2}/V = J_{kO_2} \cdot \Delta_k F_{O_2}$$

$\Delta_k F_{O_2}$ is the exergonic input force with a negative sign, and, $\Delta_m F_{H+pos}$, is the endergonic output force with a positive sign (**Box 4**). Ergodynamic efficiency is the ratio of output/input power, or the flux ratio times force ratio (Gnaiger 1993a,b),

$$\varepsilon = \frac{P_{mH^+pos}}{-P_{kO_2}} = \frac{J_{mH^+pos}}{J_{kO_2}} \cdot \frac{\Delta_m F_{H^+pos}}{-\Delta_k F_{O_2}}$$

The concept of incomplete coupling relates exclusively to the first term, *i.e.*, the flux ratio, or $H^+_{pos}/O_2$ ratio (**Fig. 1**). Likewise, respirometric definitions of the P»/O$_2$ ratio and biochemical coupling efficiency (Section 2.2) consider flux ratios. In a completely coupled process, the power efficiency, $\varepsilon$, depends entirely on the force ratio, ranging from zero efficiency at an output force of zero, to the limiting output force and maximum efficiency of 1.0, when the total power of the coupled process (the negative dissipation function), $P_t = P_{kO_2} + P_{mH+pos}$, equals zero, and any net flows are zero at ergodynamic equilibrium of a coupled process. Thermodynamic equilibrium is defined as the state when all potentials (all forces) are dissipated and equilibrate towards their minima of zero. In a fully or completely coupled process, output and input fluxes are directly proportional in a fixed ratio technically defined as a stoichiometric relationship (a gear ratio in a mechanical system). Such maximal stoichiometric output/input flux ratios are considered in OXPHOS analysis as the upper limits or mechanistic $H^+_{pos}/O_2$ and P»/O$_2$ ratios (**Fig. 1**).

---

**Coupled versus bound processes:** Since the chemiosmotic theory describes the mechanisms of coupling in OXPHOS, it may be interesting to ask if the electric and chemical parts of proton translocation are coupled processes. This is not the case according to the definition of coupling. If the coupling mechanism is disengaged, the output process becomes

independent of the input process, and both proceed in their downhill (exergonic) direction (**Fig. 2**). It is not possible to physically uncouple the electric and chemical processes, which are only *theoretically* partitioned as electric and chemical components. The electric and chemical partial protonmotive *forces*, $\Delta_{el}F_{H+}$ and $\Delta_dF_{H+}$, can be measured separately. In contrast, the corresponding proton *flux*, $J_{mH+}$, is non-separable, *i.e.*, cannot be uncoupled. Then these are not *coupled* processes, but are defined as *bound* processes. The electrical and chemical parts are tightly bound partial forces, since the flux cannot be partitioned (**Table 4**).

*3.3. Absolute and relative measurements of the protonmotive force*

Lipophilic cationic probes and ion selective electrodes are most commonly used to measure $\Delta \ln c_{Bz}$ (**Box 2**) as a basis for calculating the electric part of the protonmotive force (Canton *et al.* 1995; Rottenberg, 1984; Divakaruni and Brand 2011; Nicholls and Ferguson 2013). The radioactive rubidium isotope is considered to provide the most reliable results on the partitioning between the matrix outer compartments (Rottenberg, 1984), although the non-localized (Mitchell 2011) versus localized models remain open for discussion (Kell 1979). The mitochondrial matrix volume needs to be known either by direct measurement, or by reference to a range from 1 to 2 µL/mg mt-protein. Measurement of mt-protein requires purification of mitochondria. Corrections are required for unspecific binding of lipophilic cationic probes. In mammalian isolated mitochondria the contribution of ΔpH to the protonmotive force is relatively small under typical experimental conditions (*e.g.*, 10 mM $P_i$). ΔpH can be fully collapsed by nigericin (Canton *et al.* 1995). Fluorescent probes are widely used as indicators of mitochondrial membrane potential[§] differences, and the signals can be converted from relative to absolute values of the protonmotive force (Scaduto and Grotyohann 1999).

The chemical part of the protonmotive force is calculated from ΔpH (**Box 2**), measured with the use of radioactively labelled compounds (Canton *et al.* 1995).

## 4. Normalization: fluxes and flows

*4.1. Normalization: system or sample*

The term *rate* is not sufficiently defined to be useful for a database (**Fig. 9**). The inconsistency of the meanings of rate becomes fully apparent when considering Galileo Galilei's famous principle, that 'bodies of different weight all fall at the same rate (have a constant acceleration)' (Coopersmith 2010).

**Fig. 9. Different meanings of *rate* may lead to confusion, if the normalization is not sufficiently specified.** Results are frequently expressed as mass-specific *flux*, $J_{mX}$, per mg protein, dry or wet weight (mass). Cell volume, $V_{cell}$, may be used for normalization (volume-specific flux, $J_{Vcell}$), which must be clearly distinguished from flow per cell, $I_{Ncell}$, or flux, $J_V$, expressed for methodological reasons per volume of the measurement system. For details see **Table 7**.
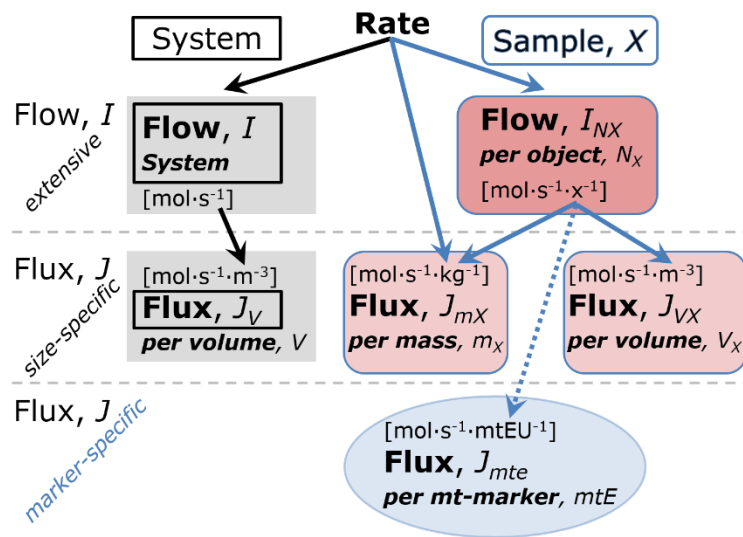
1278      **Flow per system, $I$:** In a generalization of electrical terms, flow as an extensive quantity
1279   ($I$; per system) is distinguished from flux as a size-specific quantity ($J$; per system size) (**Fig.**
1280   **9**). Electric current is flow, $I_{el}$ [A ≡ C·s$^{-1}$] per system (extensive quantity). When dividing this
1281   extensive quantity by system size (cross-sectional area of a 'wire'), a size-specific quantity is
1282   obtained, which is flux (current density), $J_{el}$ [A·m$^{-2}$ = C·s$^{-1}$·m$^{-2}$] (**Box 3**).
1283      **Extensive quantities:** An extensive quantity increases proportionally with system size.
1284   The magnitude of an extensive quantity is completely additive for non-interacting subsystems,
1285   such as mass or flow expressed per defined system. The magnitude of these quantities depends
1286   on the extent or size of the system (Cohen *et al.* 2008).
1287      **Size-specific quantities:** 'The adjective *specific* before the name of an extensive quantity
1288   is often used to mean *divided by mass*' (Cohen *et al.* 2008). In this system-paradigm, mass-
1289   specific flux is flow divided by mass of the *system* (the total mass of everything within the
1290   measuring chamber or reactor). A mass-specific quantity is independent of the extent of non-
1291   interacting homogenous subsystems. Tissue-specific quantities (related to the *sample* in
1292   contrast to the *system*) are of fundamental interest in comparative mitochondrial physiology,
1293   where *specific* refers to the *type of the sample* rather than *mass of the system*. The term *specific*,
1294   therefore, must be clarified; *sample*-specific, *e.g.*, muscle mass-specific normalization is
1295   distinguished from *system*-specific quantities (mass or volume; **Fig. 9**).
1296      **Molar quantities:** 'The adjective *molar* before the name of an extensive quantity
1297   generally means *divided by amount of substance*' (Cohen *et al.* 2008). The notion that all molar
1298   quantities then become *intensive* causes ambiguity in the meaning of *molar Gibbs energy*. It is
1299   important to emphasize the fundamental difference between normalization for amount of
1300   substance *in a system* or for amount of motive substance *in a transformation*. When the Gibbs
1301   energy of a system, $G$ [J], is divided by the amount of substance B in the system, $n_B$ [mol], a
1302   *size-specific* molar quantity is obtained, $G_B = G/n_B$ [J·mol$^{-1}$], which is not any force at all. In
1303   contrast, when the partial Gibbs energy change, $\partial G$ [J], is divided by the motive amount of
1304   substance B in reaction r (advancement of reaction), $\partial_r \xi_B$ [mol], the resulting intensive molar
1305   quantity, $\Delta_r F_B = \partial G/\partial_r \xi_B$ [J·mol$^{-1}$], is the chemical motive force of reaction r involving 1 mol B
1306   (**Table 6**, Note 4). These considerations apply not only to the molar format (**Fig. 8**).
1307
1308   *4.2. Normalization for system-size: flux per chamber volume*
1309
1310      **System-specific flux, $J_{V,O_2}$:** The experimental system (the experimental chamber) is part
1311   of the measurement apparatus, separated from the environment as an isolated, closed, open,
1312   isothermal or non-isothermal system (**Table 7**). On another level, we distinguish between (*1*)
1313   the *system* with volume $V$ and mass $m$ defined by the system boundaries, and (*2*) the *sample* or
1314   *objects* with volume $V_X$ and mass $m_X$ which are enclosed in the experimental chamber (**Fig. 9**).
1315   Metabolic $O_2$ flow per object, $I_{O_2/X}$, increases as the mass of the object is increased. Sample
1316   mass-specific $O_2$ flux, $J_{O_2/mX}$ should be independent of the mass of the smaple studied in the
1317   instrument chamber, but system volume-specific $O_2$ flux, $J_{V,O_2}$ (per volume of the instrument
1318   chamber), should increase in direct proportion to the mass of the object in the chamber. Whereas
1319   $J_{V,O_2}$ depends on mass-concentration of the sample in the chamber, it should be independent of
1320   the chamber (system) volume at constant sample mass. There are practical limitations to
1321   increase the mass-concentration of the sample in the chamber, when one is concerned about
1322   crowding effects and instrumental time resolution.
1323      When the reactor volume does not change during the reaction, which is typical for liquid
1324   phase reactions, the volume-specific *flux of a chemical reaction* r is the time derivative of the
1325   advancement of the reaction per unit volume, $J_{V,rB} = d_r\xi_B/dt·V^{-1}$ [(mol·s$^{-1}$)·L$^{-1}$]. The *rate of*
1326   *concentration change* is $dc_B/dt$ [(mol·L$^{-1}$)·s$^{-1}$], where concentration is $c_B = n_B/V$. There is a
1327   difference between (*1*) $J_{V,rO_2}$ [mol·s$^{-1}$·L$^{-1}$] and (*2*) rate of concentration change [mol·L$^{-1}$·s$^{-1}$].
1328   These merge to a single expression only in closed systems. In open systems, external fluxes

1329 (such as $O_2$ supply) are distinguished from internal transformations (metabolic flux, $O_2$
1330 consumption). In a closed system, external flows of all substances are zero and $O_2$ consumption
1331 (internal flow of catabolic reactions k), $I_{kO_2}$ [pmol·s⁻¹], causes a decline of the amount of $O_2$ in
1332 the system, $n_{O_2}$ [nmol]. Normalization of these quantities for the volume of the system, $V$ [L $\equiv$
1333 dm³], yields volume-specific $O_2$ flux, $J_{V,kO_2} = I_{kO_2}/V$ [nmol·s⁻¹·L⁻¹], and $O_2$ concentration, [$O_2$]
1334 or $c_{O_2} = n_{O_2}/V$ [μmol·L⁻¹ = μM = nmol·mL⁻¹]. Instrumental background $O_2$ flux is due to external
1335 flux into a non-ideal closed respirometer; then total volume-specific flux has to be corrected for
1336 instrumental background $O_2$ flux—$O_2$ diffusion into or out of the instrumental chamber. $J_{V,kO_2}$
1337 is relevant mainly for methodological reasons and should be compared with the accuracy of
1338 instrumental resolution of background-corrected flux, *e.g.*, ±1 nmol·s⁻¹·L⁻¹ (Gnaiger 2001).
1339 'Metabolic' or catabolic indicates $O_2$ flux, $J_{kO_2}$, corrected for: (*1*) instrumental background $O_2$
1340 flux; (*2*) chemical background $O_2$ flux due to autoxidation of chemical components added to
1341 the incubation medium; and (*3*) *Rox* for $O_2$-consuming side reactions unrelated to the catabolic
1342 pathway k.

*4.3. Normalization: per sample*

1346     The challenges of measuring mitochondrial respiratory flux are matched by those of
1347 normalization. Application of common and generally defined units is required for direct transfer
1348 of reported results into a database. The second [s] is the *SI* unit for the base quantity *time*. It is
1349 also the standard time-unit used in solution chemical kinetics. A rate may be considered as the
1350 numerator and normalization as the complementary denominator, which are tightly linked in
1351 reporting the measurements in a format commensurate with the requirements of a database.
1352 MU-formats are simply converted to different *SI* units on the basis of physical constants (**Fig.
1353 8**). In contrast, normalization (**Table 7**) is guided by physicochemical principles (**Fig. 9**),
1354 methodological considerations (**Fig. 10**), and conceptual strategies (**Fig. 11**).
1355     **Sample concentration, $C_{mX}$:** Normalization for sample concentration is required for
1356 reporting respiratory data. Consider a tissue or cells as the sample, $X$, and the sample mass, $m_X$
1357 [mg] from which a mitochondrial preparation is obtained. $m_X$ is frequently measured as wet or
1358 dry weight, $W_w$ or $W_d$ [mg], or as amount of tissue or cell protein, $m_{Protein}$. In the case of
1359 permeabilized tissues, cells, and homogenates, the sample concentration, $C_{mX} = m_X/V$ [mg·mL⁻¹
1360 = g·L⁻¹], is simply the mass of the subsample of tissue that is transferred into the instrument
1361 chamber.
1362     **Mass-specific flux, $J_{O_2/mX}$:** Mass-specific flux is obtained by expressing respiration per
1363 mass of sample, $m_X$ [mg]. $X$ is the type of sample, *e.g.*, tissue homogenate, permeabilized fibres
1364 or cells. Volume-specific flux is divided by mass concentration of $X$, $J_{O_2/mX} = J_{V,O_2}/C_{mX}$; or flow
1365 per cell is divided by mass per cell, $J_{O_2/mcell} = I_{O_2/cell}/M_{cell}$. If mass-specific $O_2$ flux is constant
1366 and independent of sample size (expressed as mass), then there is no interaction between the
1367 subsystems. A 1.5 mg and a 3.0 mg muscle sample respires at identical mass-specific flux.
1368 Mass-specific $O_2$ flux, however, may change with the mass of a tissue sample, cells or isolated
1369 mitochondria in the measuring chamber, in which case the nature of the interaction becomes an
1370 issue. Optimization of cell density and arrangement is generally important and particularly in
1371 experiments carried out in wells, considering the confluency of the cell monolayer or clumps
1372 of cells (Salabei *et al.* 2014).
1373     **Number concentration, $C_{NX}$:** $C_{NX}$ is the experimental *number concentration* of sample
1374 $X$. In the case of cells or animals, *e.g.*, nematodes, $C_{NX} = N_X/V$ [x·L⁻¹], where $N_X$ is the number
1375 of cells or organisms in the chamber (**Table 7**).
1376     **Flow per object, $I_{O_2/X}$:** A special case of normalization is encountered in respiratory
1377 studies with permeabilized (or intact) cells. If respiration is expressed per cell, the $O_2$ flow per
1378 measurement system is replaced by the $O_2$ flow per cell, $I_{O_2/cell}$ (**Table 7**). $O_2$ flow can be
1379 calculated from volume-specific $O_2$ flux, $J_{V,O_2}$ [nmol·s⁻¹·L⁻¹] (per $V$ of the measurement chamber

[L]), divided by the number concentration of cells, $C_{Nce} = N_{ce}/V$ [cell·L$^{-1}$], where $N_{ce}$ is the number of cells in the chamber. Cellular O$_2$ flow can be compared between cells of identical size. To take into account changes and differences in cell size, further normalization is required to obtain cell size-specific or mitochondrial marker-specific O$_2$ flux (Renner *et al.* 2003).

The complexity changes when the sample is a whole organism studied as an experimental model. The well-established scaling law in respiratory physiology reveals a strong interaction of O$_2$ consumption and individual body mass of an organism, since *basal* metabolic rate (flow) does not increase linearly with body mass, whereas *maximum* mass-specific O$_2$ flux, $\dot{V}_{O2max}$ or $\dot{V}_{O2peak}$, is approximately constant across a large range of individual body mass (Weibel and Hoppeler 2005), with individuals, breeds, and certain species deviating substantially from this general relationship. $\dot{V}_{O2peak}$ of human endurance athletes is 60 to 80 mL O$_2$·min$^{-1}$·kg$^{-1}$ body mass, converted to $J_{O2peak/M}$ of 45 to 60 nmol·s$^{-1}$·g$^{-1}$ (Gnaiger 2014; **Table 9**).

## Table 7. Sample concentrations and normalization of flux.

| Expression | Symbol | Definition | Unit | Notes |
|---|---|---|---|---|
| **Sample** | | | | |
| identity of sample | $X$ | object: cell, tissue, animal, patient | | |
| number of sample entities $X$ | $N_X$ | number of objects | x | |
| mass of sample $X$ | $m_X$ | | kg | 1 |
| mass of object $X$ | $M_X$ | $M_X = m_X \cdot N_X^{-1}$ | kg·x$^{-1}$ | 1 |
| **Mitochondria** | | | | |
| Mitochondria | mt | $X = \text{mt}$ | | |
| amount of mt-elements | $mtE$ | quantity of mt-marker | mtEU | |
| **Concentrations** | | | | |
| object number concentration | $C_{NX}$ | $C_{NX} = N_X \cdot V^{-1}$ | x·m$^{-3}$ | 2 |
| sample mass concentration | $C_{mX}$ | $C_{mX} = m_X \cdot V^{-1}$ | kg·m$^{-3}$ | |
| mitochondrial concentration | $C_{mtE}$ | $C_{mtE} = mtE \cdot V^{-1}$ | mtEU·m$^{-3}$ | 3 |
| specific mitochondrial density | $D_{mtE}$ | $D_{mtE} = mtE \cdot m_X^{-1}$ | mtEU·kg$^{-1}$ | 4 |
| mitochondrial content, $mtE$ per object $X$ | $mtE_X$ | $mtE_X = mtE \cdot N_X^{-1}$ | mtEU·x$^{-1}$ | 5 |
| **O$_2$ flow and flux** | | | | 6 |
| flow, system | $I_{O2}$ | internal flow | mol·s$^{-1}$ | 7 |
| volume-specific flux | $J_{V,O2}$ | $J_{V,O2} = I_{O2} \cdot V^{-1}$ | mol·s$^{-1}$·m$^{-3}$ | 8 |
| flow per object $X$ | $I_{O2/X}$ | $I_{O2/X} = J_{V,O2} \cdot C_{NX}^{-1}$ | mol·s$^{-1}$·x$^{-1}$ | 9 |
| mass-specific flux | $J_{O2/mX}$ | $J_{O2/mX} = J_{V,O2} \cdot C_{mX}^{-1}$ | mol·s$^{-1}$·kg$^{-1}$ | |
| mitochondria-specific flux | $J_{O2/mtE}$ | $J_{O2/mtE} = J_{V,O2} \cdot C_{mtE}^{-1}$ | mol·s$^{-1}$·mtEU$^{-1}$ | 10 |

1 The *SI* prefix k is used for the SI base unit of mass (kg = 1,000 g). In praxis, various *SI* prefixes are used for convenience, to make numbers easily readable, *e.g.* 1 mg tissue, cell or mitochondrial mass instead of 0.000001 kg.

2 In case sample $X$ = cells, the object number concentration is $C_{Ncell} = N_{cell} \cdot V^{-1}$, and volume may be expressed in [dm$^3$ ≡ L] or [cm$^3$ = mL]. See **Table 8** for different object types.

3 mt-concentration is an experimental variable, dependent on sample concentration: (*1*) $C_{mtE} = mtE \cdot V^{-1}$; (*2*) $C_{mtE} = mtE_X \cdot C_{NX}$; (*3*) $C_{mtE} = C_{mX} \cdot D_{mtE}$.

4 If the amount of mitochondria, $mtE$, is expressed as mitochondrial mass, then $D_{mtE}$ is the mass fraction of mitochondria in the sample. If $mtE$ is expressed as mitochondrial volume, $V_{mt}$, and the mass of sample, $m_X$, is replaced by volume of sample, $V_X$, then $D_{mtE}$ is the volume fraction of mitochondria in the sample.

1406  5  $mtE_X = mtE \cdot N_X^{-1} = C_{mtE} \cdot C_{NX}^{-1}$.

1407  6  $O_2$ can be replaced by other chemicals B to study different reactions, *e.g.* ATP, $H_2O_2$, or
1408     compartmental translocations, *e.g.* $Ca^{2+}$.

1409  7  $I_{O_2}$ and $V$ are defined per instrument chamber as a system of constant volume (and constant
1410     temperature), which may be closed or open. $I_{O_2}$ is abbreviated for $I_{rO_2}$, *i.e.*, the metabolic or internal
1411     $O_2$ flow of the chemical reaction r in which $O_2$ is consumed, hence the negative stoichiometric
1412     number, $v_{O_2} = -1$. $I_{rO_2} = d_r n_{O_2}/dt \cdot v_{O_2}^{-1}$. If r includes all chemical reactions in which $O_2$ participates, then
1413     $d_r n_{O_2} = dn_{O_2} - d_e n_{O_2}$, where $dn_{O_2}$ is the change in the amount of $O_2$ in the instrument chamber and $d_e n_{O_2}$
1414     is the amount of $O_2$ added externally to the system. At steady state, by definition $dn_{O_2} = 0$, hence $d_r n_{O_2}$
1415     $= -d_e n_{O_2}$.

1416  8  $J_{V,O_2}$ is an experimental variable, expressed per volume of the instrument chamber.

1417  9  $I_{O_2/X}$ is a physiological variable, depending on the size of entity $X$.

1418  10 There are many ways to normalize for a mitochondrial marker, that are used in different experimental
1419     approaches: (*1*) $J_{O_2/mtE} = J_{V,O_2} \cdot C_{mtE}^{-1}$; (*2*) $J_{O_2/mtE} = J_{V,O_2} \cdot C_{mX}^{-1} \cdot D_{mtE}^{-1} = J_{O_2/mX} \cdot D_{mtE}^{-1}$; (*3*) $J_{O_2/mtE} =$
1420     $J_{V,O_2} \cdot C_{NX}^{-1} \cdot mtE_X^{-1} = I_{O_2/X} \cdot mtE_X^{-1}$; (*4*) $J_{O_2/mtE} = I_{O_2} \cdot mtE^{-1}$. The mt-elemental unit [mtEU] varies between
1421     different mt-markers.

1423  **Table 8. Sample types, *X*, abbreviations, and quantification.**

| Identity of sample | $X$ | $N_X$ | Mass[a] | Volume | mt-Marker |
| --- | --- | --- | --- | --- | --- |
| mitochondrial preparation | mtprep | [x] | [kg] | [m$^3$] | [mtEU] |
| isolated mitochondria | imt | | $m_{mt}$ | $V_{mt}$ | $mtE$ |
| tissue homogenate | thom | | $m_{thom}$ | | $mtE_{thom}$ |
| permeabilized tissue | pti | | $m_{pti}$ | | $mtE_{pti}$ |
| permeabilized fibre | pfi | | $m_{pfi}$ | | $mtE_{pfi}$ |
| permeabilized cell | pce | $N_{pce}$ | $M_{pce}$ | $V_{pce}$ | $mtE_{pce}$ |
| intact cell | ce | $N_{ce}$ | $M_{ce}$ | $V_{ce}$ | $mtE_{ce}$ |
| Organism | org | $N_{org}$ | $M_{org}$ | $V_{org}$ | |

1424  [a] Instead of mass, frequently the wet weight or dry weight is stated, $W_w$ or $W_d$.
1425     $m_X$ is mass of the sample [kg], $M_X$ is mass of the object [kg·x$^{-1}$].

1427  *4.4. Normalization for mitochondrial content*

1429     Tissues can contain multiple cell populations which may have distinct mitochondrial
1430  subtypes. Mitochondria undergo dynamic fission and fusion cycles, and can exist in multiple
1431  stages and sizes which may be altered by a range of factors. The isolation of mitochondria (often
1432  achieved through differential centrifugation) can therefore yield a subsample of the
1433  mitochondrial types present in a tissue, dependent on isolation protocols utilized (*e.g.*
1434  centrifugation speed). This possible artefact should be taken into account when planning
1435  experiments using isolated mitochondria. The tendency for mitochondria of specific sizes to be
1436  enriched at different centrifugation speeds also has the potential to allow the isolation of specific
1437  mitochondrial subpopulations and therefore the analysis of mitochondria from multiple cell
1438  lineages within a single tissue.

1439     Part of the mitochondria from the tissue is lost during preparation of isolated
1440  mitochondria. The fraction of mitochondria obtained is expressed as mitochondrial recovery
1441  (**Fig. 10**). At a high mitochondrial recovery the sample of isolated mitochondria is more
1442  representative of the total mitochondrial population than in preparations characterized by low
1443  recovery. Determination of the mitochondrial recovery and yield is based on measurement of
1444  the concentration of a mitochondrial marker in the tissue homogenate, $C_{mtE,thom}$, which
1445  simultaneously provides information on the specific mitochondrial density in the sample (**Fig.
1446  10**).

1447     Normalization is a problematic subject and it is essential to consider the question of the
1448  study. If the study aims to compare tissue performance, such as the effects of a certain treatment
1449  on a specific tissue, then normalization can be successful, using tissue mass or protein content,
1450  for example. If the aim, however, is to find differences of mitochondrial function independent

of mitochondrial density (**Table 7**), then normalization to a mitochondrial marker is imperative (**Fig. 11**). However, one cannot assume that quantitative changes in various markers such as mitochondrial proteins necessarily occur in parallel with one another. It is important to first establish that the marker chosen is not selectively altered by the performed treatment. In conclusion, the normalization must reflect the question under investigation to reach a satisfying answer. On the other hand, the goal of comparing results across projects and institutions requires some standardization on normalization for entry into a databank.
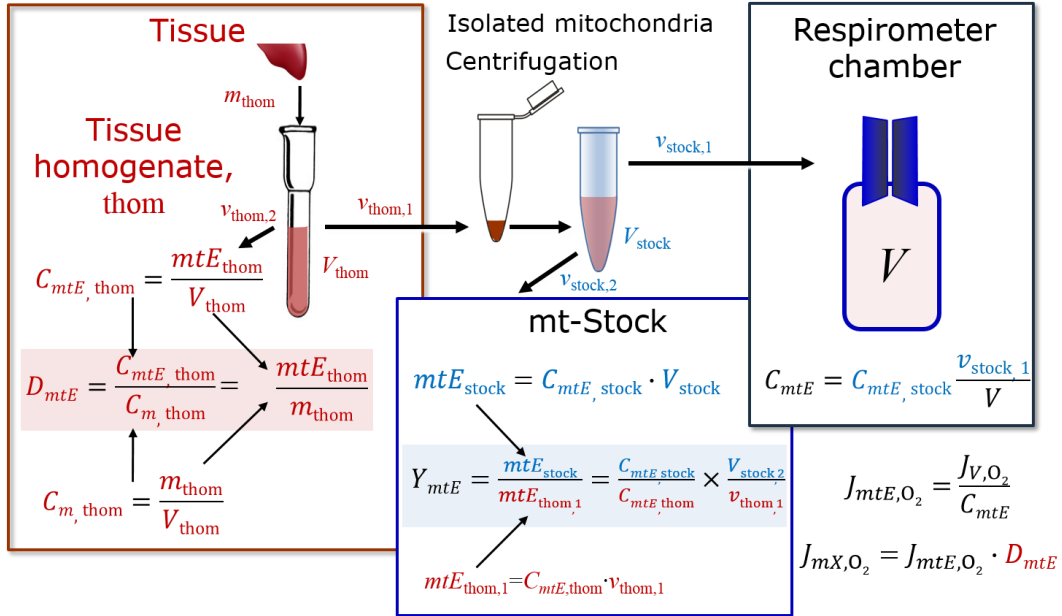


| Symbol | Definition [Units] |
|--------|--------------------|
| $C_{mtE}$ | mitochondrial concentration in chamber [mtEU·L$^{-1}$] |
| $C_m$ | sample mass concentration in chamber [g·L$^{-1}$] |
| $D_{mtE}$ | specific mte-density per tissue mass [mtEU·g$^{-1}$] |
| $J_{m,O_2}$ | mass-specific O$_2$ flux [nmol·s$^{-1}$·g$^{-1}$] |
| $J_{mtE,O_2}$ | mitochondria-specific O$_2$ flux [nmol·s$^{-1}$·mtEU$^{-1}$] |
| $mtE$ | amount of mitochondrial elements [mtEU] |
| $m_{thom}$ | mass of tissue in the homogenate [g] |
| $Y_{mtE}$ | recovery of isolated mitochondria |
| $Y_{mtE/m}$ | yield of isolated mitochondria; $Y_{mtE/m} = Y_{mtE} \cdot D_{mtE}$ [mtEU·g$^{-1}$] |
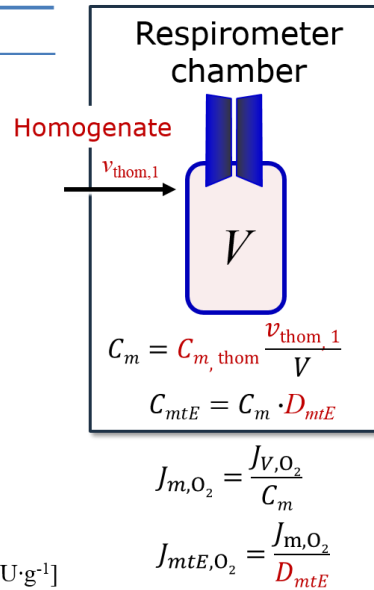
**Fig. 10. Normalization of volume-specific flux of isolated mitochondria and tissue homogenate. A:** Recovery, $Y_{mtE}$, in preparation of isolated mitochondria. $v_{thom,1}$ and $v_{stock,1}$ are the volumes transferred from the total volume, $V_{thom}$ and $V_{stock}$, respectively. $mtE_{thom,1}$ is the amount of mitochondrial elements in volume $v_{thom,1}$ used for isolation. **B:** Homogenate, $v_{thom,1}$ is transferred directly into the respirometer chamber. See **Table 7** for further symbols.

**Mitochondrial concentration, $C_{mtE}$, and mitochondrial markers:** It is important that mitochondrial concentration in the tissue and the measurement chamber be quantified, as a physiological output that is the result of mitochondrial biogenesis and degradation, and as a quantity for normalization in functional analyses. Mitochondrial organelles comprise a dynamic

1472 cellular reticulum in various states of fusion and fission. Hence the definition of an "amount"
1473 of mitochondria is often misconceived: mitochondria cannot be counted reliably as a number
1474 of occurring elements. Therefore, quantification of the "amount" of mitochondria depends on
1475 measurement of chosen mitochondrial markers. 'Mitochondria are the structural and functional
1476 elemental units of cell respiration' (Gnaiger 2014). The quantity of a mitochondrial marker can
1477 be considered to reflect the amount of *mitochondrial elements*, *mtE*, expressed in various
1478 mitochondrial elemental units [mtEU] specific for each measured mt-marker (**Table 7**).
1479 However, since mitochondrial quality changes under certain stimuli, particularly in
1480 mitochondrial dysfunction and after exercise training (Pesta *et al.* 2011; Campos *et al.* 2017),
1481 some markers can vary while other markers are unchanged: (*1*) Mitochondrial volume and
1482 membrane area are structural markers, whereas mitochondrial protein mass is frequently used
1483 as a marker for isolated mitochondria. (*2*) Molecular and enzymatic mitochondrial markers
1484 (amounts or activities) can be selected as matrix markers, *e.g.*, citrate synthase activity, mtDNA;
1485 mtIM-markers, *e.g.*, cytochrome *c* oxidase activity, $aa_3$ content, cardiolipin, or mtOM-markers,
1486 *e.g.*, TOM20. (*3*) Extending the measurement of mitochondrial marker enzyme activity to
1487 mitochondrial pathway capacity, ET- or OXPHOS-capacity can be considered as an integrative
1488 functional mitochondrial marker.
1489



1490
1491 **Fig. 11. Structure-function analysis of performance of an organism, organ or tissue, or a**
1492 **cell (sample object, *X*). O₂ flow, $I_{O_2/X}$, is the product of performance per functional element**
1493 **(element function, mitochondria-specific flux), element density (mitochondrial density,**
1494 **$D_{mtE}$), and size of entity *X* (mass, $M_X$). (A)** Structured analysis: performance is the product of
1495 mitochondrial *function* (mt-specific flux) and *structure* (functional elements; $D_{mtE}$ times mass
1496 of *X*). (**B**) Unstructured analysis: performance is the product of *entity mass-specific flux*, $J_{O_2/MX}$
1497 = $I_{O_2/X}/M_X$ = $I_{O_2}/m_X$ [mol·s⁻¹·kg⁻¹] and *size of entity*, expressed as mass of *X*; $M_X = m_X·N_X^{-1}$
1498 [kg·x⁻¹]. See **Table 7** for further explanation of quantities and units. Modified from Gnaiger
1499 (2014).
1500

1501    Depending on the type of mitochondrial marker, the mitochondrial elements, *mtE*, are
1502 expressed in marker-specific units. It is recommended to distinguish *experimental*
1503 *mitochondrial concentration*, $C_{mtE} = mtE/V$ and *physiological mitochondrial density*, $D_{mtE} =$
1504 $mtE/m_X$. Then mitochondrial density is the amount of mitochondrial elements per mass of tissue,

1505 which is a biological varible (**Fig. 11**). The experimental variable is mitochondrial density
1506 multiplied by sample mass concentration in the measuring chamber, $C_{mtE} = D_{mtE} \cdot C_{mX}$, or
1507 mitochondrial content multiplied by sample number concentration, $C_{mtE} = mtE_X \cdot C_{NX}$ (**Table 7**).
1508       **Mitochondria-specific flux, $J_{O_2/mtE}$**: Volume-specific metabolic $O_2$ flux depends on: (*1*)
1509 the sample concentration in the volume of the instrument chamber, $C_{mX}$, or $C_{NX}$; (*2*) the
1510 mitochondrial density in the sample, $D_{mtE} = mtE/m_X$ or $mtE_X = mtE/N_X$; and (*3*) the specific
1511 mitochondrial activity or performance per elemental mitochondrial unit, $J_{O_2/mtE} = J_{V,O_2}/C_{mtE}$
1512 [mol·s$^{-1}$·mtEU$^{-1}$] (**Table 7**). Obviously, the numerical results for $J_{O_2/mtE}$ vary according to the
1513 type of mitochondrial marker chosen for measurement of $mtE$ and $C_{mtE} = mtE/V$ [mtEU·m$^{-3}$].

1514

1515 *4.5. Evaluation of mitochondrial markers*

1516

1517       Different methods are implicated in quantification of mitochondrial markers and have
1518 different strengths. Some problems are common for all mitochondrial markers, $mtE$: (*1*)
1519 Accuracy of measurement is crucial, since even a highly accurate and reproducible
1520 measurement of $O_2$ flux results in an inaccurate and noisy expression normalized for a biased
1521 and noisy measurement of a mitochondrial marker. This problem is acute in mitochondrial
1522 respiration because the denominators used (the mitochondrial markers) are often very small
1523 moieties whose accurate and precise determination is difficult. This problem can be avoided
1524 when $O_2$ fluxes measured in substrate-uncoupler-inhibitor titration protocols are normalized for
1525 flux in a defined respiratory reference state, which is used as an *internal* marker and yields flux
1526 control ratios, *FCR*s (**Fig. 9**). *FCR*s are independent of any *externally* measured markers and,
1527 therefore, are statistically very robust, considering the limitations of ratios in general (Jasienski
1528 and Bazzaz 1999). *FCR*s indicate qualitative changes of mitochondrial respiratory control, with
1529 highest quantitative resolution, separating the effect of mitochondrial density or concentration
1530 on $J_{O_2/mX}$ and $I_{O_2/X}$ from that of function per elemental mitochondrial marker, $J_{O_2/mtE}$ (Pesta *et al.*
1531 2011; Gnaiger 2014). (*2*) If mitochondrial quality does not change and only the amount of
1532 mitochondria varies as a determinant of mass-specific flux, any marker is equally qualified in
1533 principle; then in practice selection of the optimum marker depends only on the accuracy and
1534 precision of measurement of the mitochondrial marker. (*3*) If mitochondrial flux control ratios
1535 change, then there may not be any best mitochondrial marker. In general, measurement of
1536 multiple mitochondrial markers enables a comparison and evaluation of normalization for a
1537 variety of mitochondrial markers. Particularly during postnatal development, the activity of
1538 marker enzymes, such as cytochrome *c* oxidase and citrate synthase, follows different time
1539 courses (Drahota *et al.* 2004). Evaluation of mitochondrial markers in healthy controls is
1540 insufficient for providing guidelines for application in the diagnosis of pathological states and
1541 specific treatments.
1542       In line with the concept of the respiratory control ratio (Chance and Williams 1955a), the
1543 most readily used normalization is that of flux control ratios and flux control factors (Gnaiger
1544 2014). Selection of the state of maximum flux in a protocol as the reference state has the
1545 advantages of: (*1*) internal normalization; (*2*) statistical linearization of the response in the range
1546 of 0 to 1; and (*3*) consideration of maximum flux for integrating a very large number of
1547 elemental steps in the OXPHOS- or ET-pathways. This reduces the risk of selecting a functional
1548 marker that is specifically altered by the treatment or pathology, yet increases the chance that
1549 the highly integrative pathway is disproportionately affected, *e.g.* the OXPHOS- rather than
1550 ET-pathway in case of an enzymatic defect in the phosphorylation-pathway. In this case,
1551 additional information can be obtained by reporting flux control ratios based on a reference
1552 state which indicates stable tissue-mass specific flux. Stereological determination of
1553 mitochondrial content via two-dimensional transmission electron microscopy can have
1554 limitations due to the dynamics of mitochondrial size (Meinild Lundby *et al.* 2017). Accurate

1555 determination of three-dimensional volume by two-dimensional microscopy can be both time
1556 consuming and statistically challenging (Larsen *et al.* 2012).
1557     The validity of using mitochondrial marker enzymes (citrate synthase activity, Complex
1558 I–IV amount or activity) for normalization of flux is limited in part by the same factors that
1559 apply to flux control ratios. Strong correlations between various mitochondrial markers and
1560 citrate synthase activity (Reichmann *et al.* 1985; Boushel *et al.* 2007; Mogensen *et al.* 2007)
1561 are expected in a specific tissue of healthy subjects and in disease states not specifically
1562 targeting citrate synthase. Citrate synthase activity is acutely modifiable by exercise
1563 (Tonkonogi *et al.* 1997; Leek *et al.* 2001). Evaluation of mitochondrial markers related to a
1564 selected age and sex cohort cannot be extrapolated to provide recommendations for
1565 normalization in respirometric diagnosis of disease, in different states of development and
1566 ageing, different cell types, tissues, and species. mtDNA normalised to nDNA via qPCR is
1567 correlated to functional mitochondrial markers including OXPHOS- and ET-capacity in some
1568 cases (Puntschart *et al.* 1995; Wang *et al.* 1999; Menshikova *et al.* 2006; Boushel *et al.* 2007),
1569 but lack of such correlations have been reported (Menshikova *et al.* 2005; Schultz and Wiesner
1570 2000; Pesta *et al.* 2011). Several studies indicate a strong correlation between cardiolipin
1571 content and increase in mitochondrial function with exercise (Menshikova *et al.* 2005;
1572 Menshikova *et al.* 2007; Larsen *et al.* 2012; Faber *et al.* 2014), but its use as a general
1573 mitochondrial biomarker in disease remains questionable.
1574
1575 *4.6. Conversion: units*
1576
1577     Many different units have been used to report the rate of oxygen consumption, OCR
1578 (**Table 9**). *SI* base units provide the common reference for introducing the theoretical principles
1579 (**Fig. 9**), and are used with appropriately chosen *SI* prefixes to express numerical data in the
1580 most practical format, with an effort towards unification within specific areas of application
1581 (**Table 10**). For studies of cells, we recommend that respiration be expressed, as far as possible,
1582 as: (*1*) $O_2$ flux normalized for a mitochondrial marker, for separation of the effects of
1583 mitochondrial quality and content on cell respiration (this includes *FCR*s as a normalization for
1584 a functional mitochondrial marker); (*2*) $O_2$ flux in units of cell volume or mass, for comparison
1585 of respiration of cells with different cell size (Renner *et al.* 2003) and with studies on tissue
1586 preparations, and (*3*) $O_2$ flow in units of attomole ($10^{-18}$ mol) of $O_2$ consumed in a second by
1587 each cell [$amol \cdot s^{-1} \cdot cell^{-1}$], numerically equivalent to [$pmol \cdot s^{-1} \cdot 10^{-6}$ cells]. This convention
1588 allows information to be easily used when designing experiments in which oxygen consumption
1589 must be considered. For example, to estimate the volume-specific $O_2$ flux in an instrument
1590 chamber that would be expected at a particular cell number concentration, one simply needs to
1591 multiply the flow per cell by the number of cells per volume of interest. This provides the
1592 amount of $O_2$ [mol] consumed per time [$s^{-1}$] per unit volume [$L^{-1}$]. At an $O_2$ flow of 100
1593 $amol \cdot s^{-1} \cdot cell^{-1}$ and a cell density of $10^9$ cells$\cdot L^{-1}$ ($10^6$ cells$\cdot mL^{-1}$), the volume-specific $O_2$ flux is
1594 100 $nmol \cdot s^{-1} \cdot L^{-1}$ (100 $pmol \cdot s^{-1} \cdot mL^{-1}$).
1595     Although volume is expressed as m$^3$ using the *SI* base unit, the litre [dm$^3$] is a
1596 conventional unit of volume for concentration and is used for most solution chemical kinetics.
1597 If one multiplies $I_{O_2/cell}$ by $C_{Ncell}$, then the result will not only be the amount of $O_2$ [mol]
1598 consumed per time [$s^{-1}$] in one litre [$L^{-1}$], but also the change in the concentration of oxygen per
1599 second (for any volume of an ideally closed system). This is ideal for kinetic modeling as it
1600 blends with chemical rate equations where concentrations are typically expressed in mol$\cdot L^{-1}$
1601 (Wagner *et al.* 2011). In studies of multinuclear cells, such as differentiated skeletal muscle
1602 cells, it is easy to determine the number of nuclei but not the total number of cells. A generalized
1603 concept, therefore, is obtained by substituting cells by nuclei as the sample entity. This does not
1604 hold, however, for enucleated platelets.

1605     $J_{kO_2}$ is coupled in mitochondrial steady states to proton cycling, $J_{mH+\infty} = J_{mH+pos} = J_{mH+neg}$
1606 (**Fig. 2**). $J_{mH+pos,n}$ and $J_{mH+neg,n}$ [nmol·s$^{-1}$·L$^{-1}$] are converted into electrical units, $J_{mH+pos,e}$
1607 [mC·s$^{-1}$·L$^{-1}$ = mA·L$^{-1}$] = $J_{mH+pos,n}$ [nmol·s$^{-1}$·L$^{-1}$]·$F$ [C·mol$^{-1}$]·10$^{-6}$ (**Table 4**). At a $J_{mH+pos}/J_{kO_2}$ ratio
1608 or H$^+_{pos}$/O$_2$ of 20 (H$^+_{pos}$/O = 10), a volume-specific O$_2$ flux of 100 nmol·s$^{-1}$·L$^{-1}$ would
1609 correspond to a proton flux of 2,000 nmol H$^+_{pos}$·s$^{-1}$·L$^{-1}$ or volume-specific current of 193
1610 mA·L$^{-1}$.

1611

1612 $$J_{V,mH+pos,e}\ [\text{mA·L}^{-1}] = J_{V,mH+pos,n}\ ·F·10^{-6}\ [\text{nmol·s}^{-1}·\text{L}^{-1}·\text{mC·nmol}^{-1}] \qquad (3.1)$$
1613 $$J_{V,mH+pos,e}\ [\text{mA·L}^{-1}] = J_{V,O_2}·(\text{H}^+_{pos}/\text{O}_2)·F·10^{-6}\ [\text{mC·s}^{-1}·\text{L}^{-1} = \text{mA·L}^{-1}] \qquad (3.2)$$

1614

1615 **Table 9. Conversion of various units used in respirometry and**
1616 **ergometry.** e$^-$ is the number of electrons or reducing equivalents. $z_B$ is the
1617
1618 charge number of entity B.

| 1 Unit | x | Multiplication factor | SI-Unit | Note |
|---|---|---|---|---|
| ng.atom O·s$^{-1}$ | (2 e$^-$) | 0.5 | nmol O$_2$·s$^{-1}$ | |
| ng.atom O·min$^{-1}$ | (2 e$^-$) | 8.33 | pmol O$_2$·s$^{-1}$ | |
| natom O·min$^{-1}$ | (2 e$^-$) | 8.33 | pmol O$_2$·s$^{-1}$ | |
| nmol O$_2$·min$^{-1}$ | (4 e$^-$) | 16.67 | pmol O$_2$·s$^{-1}$ | |
| nmol O$_2$·h$^{-1}$ | (4 e$^-$) | 0.2778 | pmol O$_2$·s$^{-1}$ | |
| mL O$_2$·min$^{-1}$ at STPD$^a$ | | 0.744 | µmol O$_2$·s$^{-1}$ | 1 |
| W = J/s at -470 kJ/mol O$_2$ | | -2.128 | µmol O$_2$·s$^{-1}$ | |
| mA = mC·s$^{-1}$ | ($z_{H+}$ = 1) | 10.36 | nmol H$^+$·s$^{-1}$ | 2 |
| mA = mC·s$^{-1}$ | ($z_{O_2}$ = 4) | 2.59 | nmol O$_2$·s$^{-1}$ | 2 |
| nmol H$^+$·s$^{-1}$ | ($z_{H+}$ = 1) | 0.09649 | mA | 3 |
| nmol O$_2$·s$^{-1}$ | ($z_{O_2}$ = 4) | 0.38594 | mA | 3 |

1619 1   At standard temperature and pressure dry (STPD: 0 °C = 273.15 K and 1 atm =
1620     101.325 kPa = 760 mmHg), the molar volume of an ideal gas, $V_m$, and $V_{m,O_2}$ is
1621     22.414 and 22.392 L·mol$^{-1}$ respectively. Rounded to three decimal places, both
1622     values yield the conversion factor of 0.744. For comparison at NTPD (20 °C),
1623     $V_{m,O_2}$ is 24.038 L·mol$^{-1}$. Note that the *SI* standard pressure is 100 kPa.
1624 2   The multiplication factor is $10^6/(z_B·F)$.
1625 3   The multiplication factor is $z_B·F/10^6$.

1626
1627 ET-capacity in various human cell types including HEK 293, primary HUVEC and fibroblasts
1628 ranges from 50 to 180 amol·s$^{-1}$·cell$^{-1}$, measured in intact cells in the noncoupled state (see
1629 Gnaiger 2014). At 100 amol·s$^{-1}$·cell$^{-1}$ corrected for *Rox* (corresponding to a catabolic power of
1630 -48 pW·cell$^{-1}$), the current across the mt-membranes, $I_{H+e}$, approximates 193 pA·cell$^{-1}$ or 0.2 nA
1631 per cell. See Rich (2003) for an extension of quantitative bioenergetics from the molecular to
1632 the human scale, with a transmembrane proton flux equivalent to 520 A in an adult at a catabolic
1633 power of -110 W. Modelling approaches illustrate the link between protonmotive force and
1634 currents (Willis *et al.* 2016).
1635     We consider isolated mitochondria as powerhouses and proton pumps as molecular
1636 machines to relate experimental results to energy metabolism of the intact cell. The cellular
1637 P»/O$_2$ based on oxidation of glycogen is increased by the glycolytic (fermentative) substrate-
1638 level phosphorylation of 3 P»/Glyc, *i.e.*, 0.5 mol P» for each mol O$_2$ consumed in the complete
1639 oxidation of a mol glycosyl unit (Glyc). Adding 0.5 to the mitochondrial P»/O$_2$ ratio of 5.4
1640 yields a bioenergetic cell physiological P»/O$_2$ ratio close to 6. Two NADH equivalents are
1641 formed during glycolysis and transported from the cytosol into the mitochondrial matrix, either

by the malate-aspartate shuttle or by the glycerophosphate shuttle resulting in different theoretical yields of ATP generated by mitochondria, the energetic cost of which potentially must be taken into account. Considering also substrate-level phosphorylation in the TCA cycle, this high P»/$O_2$ ratio not only reflects proton translocation and OXPHOS studied in isolation, but integrates mitochondrial physiology with energy transformation in the living cell (Gnaiger 1993a).

**Table 10. Conversion of units with preservation of numerical values.**

| Name | Frequently used unit | Equivalent unit | Note |
|---|---|---|---|
| volume-specific flux, $J_{V,O_2}$ | $pmol \cdot s^{-1} \cdot mL^{-1}$ | $nmol \cdot s^{-1} \cdot L^{-1}$ | 1 |
| | $mmol \cdot s^{-1} \cdot L^{-1}$ | $mol \cdot s^{-1} \cdot m^{-3}$ | |
| cell-specific flow, $I_{O_2/cell}$ | $pmol \cdot s^{-1} \cdot 10^{-6}$ cells | $amol \cdot s^{-1} \cdot cell^{-1}$ | 2 |
| | $pmol \cdot s^{-1} \cdot 10^{-9}$ cells | $zmol \cdot s^{-1} \cdot cell^{-1}$ | 3 |
| cell number concentration, $C_{Nce}$ | $10^6$ cells$\cdot mL^{-1}$ | $10^9$ cells$\cdot L^{-1}$ | |
| mitochondrial protein concentration, $C_{mtE}$ | $0.1$ mg$\cdot mL^{-1}$ | $0.1$ g$\cdot L^{-1}$ | |
| mass-specific flux, $J_{O_2/m}$ | $pmol \cdot s^{-1} \cdot mg^{-1}$ | $nmol \cdot s^{-1} \cdot g^{-1}$ | 4 |
| catabolic power, $P_k$ | $\mu W \cdot 10^{-6}$ cells | $pW \cdot cell^{-1}$ | 1 |
| volume | $1,000$ L | $m^3$ ($1,000$ kg) | |
| | L | $dm^3$ (kg) | |
| | mL | $cm^3$ (g) | |
| | $\mu L$ | $mm^3$ (mg) | |
| | fL | $\mu m^3$ (pg) | 5 |
| amount of substance concentration | $M = mol \cdot L^{-1}$ | $mol \cdot dm^{-3}$ | |

1  pmol: picomole = $10^{-12}$ mol    4  nmol: nanomole = $10^{-9}$ mol
2  amol: attomole = $10^{-18}$ mol    5  fL: femtolitre = $10^{-15}$ L
3  zmol: zeptomole = $10^{-21}$ mol


## 5. Conclusions

MitoEAGLE can serve as a gateway to better diagnose mitochondrial respiratory defects linked to genetic variation, age-related health risks, sex-specific mitochondrial performance, lifestyle with its effects on degenerative diseases, and thermal and chemical environment. The present recommendations on coupling control states and rates, linked to the concept of the protonmotive force, are focused on studies with mitochondrial preparations. These will be extended in a series of reports on pathway control of mitochondrial respiration, respiratory states in intact cells, and harmonization of experimental procedures.

The optimal choice for expressing mitochondrial and cell respiration (**Box 6**) as $O_2$ flow per biological system, and normalization for specific tissue-markers (volume, mass, protein) and mitochondrial markers (volume, protein, content, mtDNA, activity of marker enzymes, respiratory reference state) is guided by the scientific question under study. Interpretation of the obtained data depends critically on appropriate normalization, and therefore reporting rates merely as $nmol \cdot s^{-1}$ is discouraged, since it restricts the analysis to intra-experimental comparison of relative (qualitative) differences. Expressing $O_2$ consumption per cell may not be possible when dealing with tissues. For studies with mitochondrial preparations, we recommend that normalizations be provided as far as possible: (*1*) on a per cell basis as $O_2$ flow (a biophysical normalization); (*2*) per g cell or tissue protein, or per cell or tissue mass as mass-specific $O_2$ flux (a cellular normalization); and (*3*) per mitochondrial marker as mt-specific flux

1676 (a mitochondrial normalization). With information on cell size and the use of multiple
1677 normalizations, maximum potential information is available (Renner *et al.* 2003; Wagner *et al.*
1678 2011; Gnaiger 2014).
1679      Total mitochondrial protein is frequently applied as a mitochondrial marker restricted to
1680 isolated mitochondria. The mitochondrial recovery and yield, and experimental criteria for
1681 evaluation of purity versus integrity should be reported. Mitochondrial markers, such as citrate
1682 synthase activity as an enzymatic matrix marker, provide a link to the tissue of origin on the
1683 basis of calculating the mitochondrial recovery, *i.e.*, the fraction of mitochondrial marker
1684 obtained from a unit mass of tissue.
1685

---

1686 **Box 6: Mitochondrial and cell respiration**
1687
1688 Mitochondrial and cell respiration is the process of highly exergonic and exothermic energy
1689 transformation in which scalar redox reactions are coupled to vectorial ion translocation across
1690 a semipermeable membrane, which separates the small volume of a bacterial cell or
1691 mitochondrion from the larger volume of its surroundings. The electrochemical exergy can be
1692 partially conserved in the phosphorylation of ADP to ATP or in ion pumping, or dissipated in
1693 an electrochemical short-circuit. Respiration is thus clearly distinguished from fermentation as
1694 the counterpart of cellular core energy metabolism. Respiration is separated in mitochondrial
1695 preparations from the partial contribution of fermentative pathways of the intact cell. According
1696 to this definition, residual oxygen consumption, as measured after inhibition of mitochondrial
1697 electron transfer, does not belong to the class of catabolic reactions and is, therefore, subtracted
1698 from total oxygen consumption to obtain baseline-corrected respiration.

---

1699
1700      Molecular, molar or electrical formats can be chosen for reporting metabolic fluxes and
1701 the motive forces. The motive entities are expressed in *SI* units corresponding to these formats
1702 (pure number, mole, coulomb). The molar or chemical format, $n$, is most commonly used for
1703 reporting metabolic fluxes and concentrations in solution chemical kinetics, whereas the
1704 protonmotive force is more frequently expressed in the electrical format, $e$. The molecular or
1705 particle format, $N$, is based on counting the number of occurring elements, which is not
1706 practicable for mitochondria in their dynamic states of fusion and fission, but is standard for
1707 most cell types. A number concentration of $10^9$ cells$\cdot$L$^{-1}$ is hardly ever expressed in the molar
1708 format of 1.66 fmol cells$\cdot$L$^{-1}$. When $O_2$ flow is given as 100 amol$\cdot$s$^{-1}\cdot$cell$^{-1}$, a mixed $n/N$ format
1709 is used. $60.2\cdot10^6$ mol $O_2\cdot$s$^{-1}\cdot$mol$^{-1}$ cells is equivalent to $60.2\cdot10^6$ molecules $O_2\cdot$s$^{-1}\cdot$cell$^{-1}$ and
1710 represents a consistent $n/n$ or $N/N$ format, which is - perhaps surprisingly - not familiar and
1711 hardly ever used. The variety of formats is large and sufficiently confusing even on the basis of
1712 *SI* units. To avoid further complicating the field of mitochondrial physiology, therefore, strict
1713 adherence to *SI* units is mandatory. Furthermore, the chemical format with the motive unit *mole*
1714 has the highest chance of general acceptance in cell metabolism and mitochondrial physiology.
1715 Taken together, this evaluation provides a strong argument for a recommendation to report
1716 respiratory rates, including scalar and vectorial flows and fluxes, and states, including the
1717 protonmotive force, in a common chemical format for entry into any database. Terms and
1718 symbols are summarized in **Table 11**, the use of which is recommended for reporting results
1719 on the protonmotive force and respiratory control. This will facilitate transdisciplinary
1720 communication and support further developments towards a consistent theory of bioenergetics
1721 and mitochondrial physiology.
1722

## Table 11. Terms, symbols, and units.

| Term | Symbol | *SI* unit | Links and comments |
|------|--------|-----------|--------------------|
| alternative quinol oxidase | AOX | | Fig. 1 |
| amount of substance B | $n_B$ | [mol] | Tab. 5 |
| apparent equilibrium constant | $K_m$' | | |
| charge number | $z_B$ | | $z_B = Q_B \cdot e^{-1}$; Tab. 6; Tab. 9 |
| Complexes I to IV | CI to CIV | | respiratory ET Complexes; Fig. 1 |
| concentration of substance B | $c_B = n_B \cdot V^{-1}$; [B] | [mol·m$^{-3}$] | Box 2, Tab. 6, Section 4.1 |
| diffusion, partial component | d | | Tab. 4; chemical component |
| electric charge | $Q_{el}$ | [C] | $I_{el} = dQ_{el} \cdot dt^{-1}$ [A]; Box 3 |
| electric, partial component | el | | Tab. 4 |
| electrical format | $e$ | [C] | Fig. 8 |
| electron | e$^-$ | [x] | Tab. 9 |
| electron transfer system | ETS | | |
| elementary charge, proton charge | $e$ | [C·x$^{-1}$] | Tab. 5 |
| flow, for substance B | $I_B$ | [MU·s$^{-1}$] | system-related extensive quantity; Fig. 9 |
| flux, for substance B | $J_B$ | | size-specific quantitiy; Fig. 9, Tab. 6 |
| force, isomorphic, per B | $\Delta_{tr}F_B$ | [J·MU$^{-1}$] | Tab. 6, Box 4; force of transformation tr. tr must be defined, *e.g.*, as chemical reaction, r; diffusion, d; motion, m. |
| inorganic phosphate | $P_i$ | | |
| LEAK | LEAK | | Tab. 1 |
| mass of sample $X$ | $m_X$ | [kg] | Tab. 7 |
| mass of entity $X$ | $M_X$ | [kg] | Tab. 7 |
| MITOCARTA | | | https://www.broadinstitute.org/scientific-community/science/programs/metabolic-disease-program/publications/mitocarta/mitocarta-in-0 |
| mitochondria or mitochondrial | mt | | Box 1 |
| mitochondrial DNA | mtDNA | | Box 1 |
| mitochondrial concentration | $C_{mtE} = mtE \cdot V^{-1}$ | [mtEU·m$^{-3}$] | Tab. 7 |
| mitochondrial content | $mtE_X = mtE \cdot N_X^{-1}$ | [mtEU·x$^{-1}$] | Tab. 7 |
| mitochondrial elemental unit | mtEU | *varies* | Tab. 7, specific units for mt-marker |
| mitochondrial inner membrane | mtIM | | MIM is widely used, and M is replaced by mt as abbreviation for mitochondria; Box 1 |
| mitochondrial outer membrane | mtOM | | MOM is widely used, and M is replaced by mt as abbreviation for mitochondria; Box 1 |
| mitochondrial recovery | $Y_{mtE}$ | | Fig. 10 |
| mitochondrial yield | $Y_{mtE/m}$ | | Fig. 10 |
| molecular format | $N$ | [x] | Fig. 8 |
| molar format | $n$ | [mol] | Fig. 8 |
| motive, total | m | | Tab. 4; motive = electric + chemical |
| motive unit | MU | *varies* | Fig. 8 |
| negative | neg | | Fig. 2 |
| number concentration of $X$ | $C_{NX}$ | [x·m$^{-3}$] | Tab. 7 |
| number of entities $X$ | $N_X$ | [x] | Tab. 7, Fig. 11 |
| number of entity B | $N_B$ | [x] | Fig. 8; according to IUPAC, the unit of $N$ is "1", but the Avogadro constant, $N_A$ = $N/n$, has the IUPAC unit [mol$^{-1}$] rather than [1·mol$^{-1}$]. For consistency, we suggest the unit [x] for $N$ and [x·mol$^{-1}$] for $N_A$ (Tab. 5). |
| oxidative phosphorylation | OXPHOS | | Tab. 1 |
| oxygen concentration | $c_{O2} = n_{O2} \cdot V^{-1}$; [O$_2$] | [mol·m$^{-3}$] | Section 4.1 |
| phosphorylation of ADP to ATP | P» | | |

| | | | |
|---|---|---|---|
| positive | pos | | Fig. 2 |
| power of energy transformation, tr | $P_{tr}$ | | Tab. 6 |
| proton in the negative compartment | $H^+_{neg}$ | | Fig. 2 |
| proton in the positive compartment | $H^+_{pos}$ | | Fig. 2 |
| protonmotive force | $\Delta_m F_{H+}$ | [J·MU$^{-1}$] | Tab. 4 |
| rate of electron transfer in ET state | $E$ | | ET-capacity; Tab. 1 |
| rate of LEAK respiration | $L$ | | Tab. 1 |
| rate of oxidative phosphorylation | $P$ | | OXPHOS capacity; Tab. 1 |
| rate of residual oxygen consumption | $Rox$ | | Tab. 1 |
| residual oxygen consumption | ROX | | Tab. 1 |
| specific mitochondrial density | $D_{mtE} = mtE·m_X^{-1}$ | [mtEU·kg$^{-1}$] | Tab. 7 |
| volume | $V$ | [m$^{-3}$] | |
| weight, dry weight | $W_d$ | [kg] | used as mass of sample $X$; Fig. 9 |
| weight, wet weight | $W_w$ | [kg] | used as mass of sample $X$; Fig. 9 |

## Acknowledgements

**Competing financial interests:** E.G. is founder and CEO of Oroboros Instruments, Innsbruck, Austria.

## 6. References

Altmann R (1894) Die Elementarorganismen und ihre Beziehungen zu den Zellen. Zweite vermehrte Auflage. Verlag Von Veit & Comp, Leipzig:160 pp.

Beard DA (2005) A biophysical model of the mitochondrial respiratory system and oxidative phosphorylation. PLoS Comput Biol 1(4):e36.

Benda C (1898) Weitere Mitteilungen über die Mitochondria. Verh Dtsch Physiol Ges:376-83.

Birkedal R, Laasmaa M, Vendelin M (2014) The location of energetic compartments affects energetic communication in cardiomyocytes. Front Physiol 5:376.

Breton S, Beaupré HD, Stewart DT, Hoeh WR, Blier PU (2007) The unusual system of doubly uniparental inheritance of mtDNA: isn't one enough? Trends Genet 23:465-74.

Brown GC (1992) Control of respiration and ATP synthesis in mammalian mitochondria and cells. Biochem J 284:1-13.

Calvo SE, Klauser CR, Mootha VK (2016) MitoCarta2.0: an updated inventory of mammalian mitochondrial proteins. Nucleic Acids Research 44:D1251-7.

Calvo SE, Julien O, Clauser KR, Shen H, Kamer KJ, Wells JA, Mootha VK (2017) Comparative analysis of mitochondrial N-termini from mouse, human, and yeast. Mol Cell Proteomics 16:512-23.

Campos JC, Queliconi BB, Bozi LHM, Bechara LRG, Dourado PMM, Andres AM, Jannig PR, Gomes KMS, Zambelli VO, Rocha-Resende C, Guatimosim S, Brum PC, Mochly-Rosen D, Gottlieb RA, Kowaltowski AJ, Ferreira JCB (2017) Exercise reestablishes autophagic flux and mitochondrial quality control in heart failure. Autophagy 13:1304-317.

Canton M, Luvisetto S, Schmehl I, Azzone GF (1995) The nature of mitochondrial respiration and discrimination between membrane and pump properties. Biochem J 310:477-81.

Chance B, Williams GR (1955a) Respiratory enzymes in oxidative phosphorylation. I. Kinetics of oxygen utilization. J Biol Chem 217:383-93.

Chance B, Williams GR (1955b) Respiratory enzymes in oxidative phosphorylation: III. The steady state. J Biol Chem 217:409-27.

Chance B, Williams GR (1955c) Respiratory enzymes in oxidative phosphorylation. IV. The respiratory chain. J Biol Chem 217:429-38.

Chance B, Williams GR (1956) The respiratory chain and oxidative phosphorylation. Adv Enzymol Relat Subj Biochem 17:65-134.

Cobb LJ, Lee C, Xiao J, Yen K, Wong RG, Nakamura HK, Mehta HH, Gao Q, Ashur C, Huffman DM, Wan J, Muzumdar R, Barzilai N, Cohen P (2016) Naturally occurring mitochondrial-derived peptides are age-dependent regulators of apoptosis, insulin sensitivity, and inflammatory markers. Aging (Albany NY) 8:796-809.

Cohen ER, Cvitas T, Frey JG, Holmström B, Kuchitsu K, Marquardt R, Mills I, Pavese F, Quack M, Stohner J, Strauss HL, Takami M, Thor HL (2008) Quantities, units and smbols in physical chemistry, IUPAC Green Book, 3rd Edition, 2nd Printing, IUPAC & RSC Publishing, Cambridge.

1845 Cooper H, Hedges LV, Valentine JC, eds (2009) The handbook of research synthesis and meta-analysis. Russell
1846      Sage Foundation.
1847 Coopersmith J (2010) Energy, the subtle concept. The discovery of Feynman's blocks from Leibnitz to Einstein.
1848      Oxford University Press:400 pp.
1849 Cummins J (1998) Mitochondrial DNA in mammalian reproduction. Rev Reprod 3:172-82.
1850 Dai Q, Shah AA, Garde RV, Yonish BA, Zhang L, Medvitz NA, Miller SE, Hansen EL, Dunn CN, Price TM
1851      (2013) A truncated progesterone receptor (PR-M) localizes to the mitochondrion and controls cellular
1852      respiration. Mol Endocrinol 27:741-53.
1853 Divakaruni AS, Brand MD (2011) The regulation and physiology of mitochondrial proton leak. Physiology
1854      (Bethesda) 26:192-205.
1855 Doerrier C, Garcia-Souza LF, Krumschnabel G, Wohlfarter Y, Mészáros AT, Gnaiger E (2018) High-Resolution
1856      FluoRespirometry and OXPHOS protocols for human cells, permeabilized fibres from small biopsies of
1857      muscle and isolated mitochondria. Methods Mol. Biol. (in press)
1858 Doskey CM, van 't Erve TJ, Wagner BA, Buettner GR (2015) Moles of a substance per cell is a highly
1859      informative dosing metric in cell culture. PLOS ONE 10:e0132572.
1860 Drahota Z, Milerová M, Stieglerová A, Houstek J, Ostádal B (2004) Developmental changes of cytochrome $c$
1861      oxidase and citrate synthase in rat heart homogenate. Physiol Res 53:119-22.
1862 Duarte FV, Palmeira CM, Rolo AP (2014) The role of microRNAs in mitochondria: small players acting wide.
1863      Genes (Basel) 5:865-86.
1864 Ernster L, Schatz G (1981) Mitochondria: a historical review. J Cell Biol 91:227s-55s.
1865 Estabrook RW (1967) Mitochondrial respiratory control and the polarographic measurement of ADP:O ratios.
1866      Methods Enzymol 10:41-7.
1867 Faber C, Zhu ZJ, Castellino S, Wagner DS, Brown RH, Peterson RA, Gates L, Barton J, Bickett M, Hagerty L,
1868      Kimbrough C, Sola M, Bailey D, Jordan H, Elangbam CS (2014) Cardiolipin profiles as a potential
1869      biomarker of mitochondrial health in diet-induced obese mice subjected to exercise, diet-restriction and
1870      ephedrine treatment. J Appl Toxicol 34:1122-9.
1871 Fell D (1997) Understanding the control of metabolism. Portland Press.
1872 Garlid KD, Beavis AD, Ratkje SK (1989) On the nature of ion leaks in energy-transducing membranes. Biochim
1873      Biophys Acta 976:109-20.
1874 Garlid KD, Semrad C, Zinchenko V. Does redox slip contribute significantly to mitochondrial respiration? In:
1875      Schuster S, Rigoulet M, Ouhabi R, Mazat J-P, eds (1993) Modern trends in biothermokinetics. Plenum Press,
1876      New York, London:287-93.
1877 Gerö D, Szabo C (2016) Glucocorticoids suppress mitochondrial oxidant production via upregulation of
1878      uncoupling protein 2 in hyperglycemic endothelial cells. PLoS One 11:e0154813.
1879 Gibney E (2017) New definitions of scientific units are on the horizon. Nature 550:312–13.
1880 Gnaiger E. Efficiency and power strategies under hypoxia. Is low efficiency at high glycolytic ATP production a
1881      paradox? In: Surviving Hypoxia: Mechanisms of Control and Adaptation. Hochachka PW, Lutz PL, Sick T,
1882      Rosenthal M, Van den Thillart G, eds (1993a) CRC Press, Boca Raton, Ann Arbor, London, Tokyo:77-109.
1883 Gnaiger E (1993b) Nonequilibrium thermodynamics of energy transformations. Pure Appl Chem 65:1983-2002.
1884 Gnaiger E (2001) Bioenergetics at low oxygen: dependence of respiration and phosphorylation on oxygen and
1885      adenosine diphosphate supply. Respir Physiol 128:277-97.
1886 Gnaiger E (2009) Capacity of oxidative phosphorylation in human skeletal muscle. New perspectives of
1887      mitochondrial physiology. Int J Biochem Cell Biol 41:1837-45.
1888 Gnaiger E (2014) Mitochondrial pathways and respiratory control. An introduction to OXPHOS analysis. 4th ed.
1889      Mitochondr Physiol Network 19.12. Oroboros MiPNet Publications, Innsbruck:80 pp.
1890 Gnaiger E, Méndez G, Hand SC (2000) High phosphorylation efficiency and depression of uncoupled respiration
1891      in mitochondria under hypoxia. Proc Natl Acad Sci USA 97:11080-5.
1892 Greggio C, Jha P, Kulkarni SS, Lagarrigue S, Broskey NT, Boutant M, Wang X, Conde Alonso S, Ofori E,
1893      Auwerx J, Cantó C, Amati F (2017) Enhanced respiratory chain supercomplex formation in response to
1894      exercise in human skeletal muscle. Cell Metab 25:301-11.
1895 Hinkle PC (2005) P/O ratios of mitochondrial oxidative phosphorylation. Biochim Biophys Acta 1706:1-11.
1896 Hofstadter DR (1979) Gödel, Escher, Bach: An eternal golden braid. A metaphorical fugue on minds and
1897      machines in the spirit of Lewis Carroll. Harvester Press:499 pp.
1898 Illaste A, Laasmaa M, Peterson P, Vendelin M (2012) Analysis of molecular movement reveals latticelike
1899      obstructions to diffusion in heart muscle cells. Biophys J 102:739-48.
1900 Jasienski M, Bazzaz FA (1999) The fallacy of ratios and the testability of models in biology. Oikos 84:321-26.
1901 Jepihhina N, Beraud N, Sepp M, Birkedal R, Vendelin M (2011) Permeabilized rat cardiomyocyte response
1902      demonstrates intracellular origin of diffusion obstacles. Biophys J 101:2112-21.
1903 Kell DB (1979) On the functional proton current pathway of electron transport phosphorylation: An electrodic
1904      view. Biochim Biophys Acta 549:55-99.

Klepinin A, Ounpuu L, Guzun R, Chekulayev V, Timohhina N, Tepp K, Shevchuk I, Schlattner U, Kaambre T (2016) Simple oxygraphic analysis for the presence of adenylate kinase 1 and 2 in normal and tumor cells. J Bioenerg Biomembr 48:531-48.

Klingenberg M (2017) UCP1 - A sophisticated energy valve. Biochimie 134:19-27.

Koit A, Shevchuk I, Ounpuu L, Klepinin A, Chekulayev V, Timohhina N, Tepp K, Puurand M,Truu L, Heck K, Valvere V, Guzun R, Kaambre T (2017) Mitochondrial respiration in human colorectal and breast cancer clinical material is regulated differently. Oxid Med Cell Longev 1372640.

Komlódi T, Tretter L (2017) Methylene blue stimulates substrate-level phosphorylation catalysed by succinyl-CoA ligase in the citric acid cycle. Neuropharmacology 123:287-98.

Lane N (2005) Power, sex, suicide: mitochondria and the meaning of life. Oxford University Press:354 pp.

Larsen S, Nielsen J, Neigaard Nielsen C, Nielsen LB, Wibrand F, Stride N, Schroder HD, Boushel RC, Helge JW, Dela F, Hey-Mogensen M (2012) Biomarkers of mitochondrial content in skeletal muscle of healthy young human subjects. J Physiol 590:3349-60.

Lee C, Zeng J, Drew BG, Sallam T, Martin-Montalvo A, Wan J, Kim SJ, Mehta H, Hevener AL, de Cabo R, Cohen P (2015) The mitochondrial-derived peptide MOTS-c promotes metabolic homeostasis and reduces obesity and insulin resistance. Cell Metab 21:443-54.

Lee SR, Kim HK, Song IS, Youm J, Dizon LA, Jeong SH, Ko TH, Heo HJ, Ko KS, Rhee BD, Kim N, Han J (2013) Glucocorticoids and their receptors: insights into specific roles in mitochondria. Prog Biophys Mol Biol 112:44-54.

Leek BT, Mudaliar SR, Henry R, Mathieu-Costello O, Richardson RS (2001) Effect of acute exercise on citrate synthase activity in untrained and trained human skeletal muscle. Am J Physiol Regul Integr Comp Physiol 280:R441-7.

Lemieux H, Blier PU, Gnaiger E (2017) Remodeling pathway control of mitochondrial respiratory capacity by temperature in mouse heart: electron flow through the Q-junction in permeabilized fibers. Sci Rep 7:2840.

Lenaz G, Tioli G, Falasca AI, Genova ML (2017) Respiratory supercomplexes in mitochondria. In: Mechanisms of primary energy trasduction in biology. M Wikstrom (ed) Royal Society of Chemistry Publishing, London, UK:296-337.

Margulis L (1970) Origin of eukaryotic cells. New Haven: Yale University Press.

Meinild Lundby AK, Jacobs RA, Gehrig S, de Leur J, Hauser M, Bonne TC, Flück D, Dandanell S, Kirk N, Kaech A, Ziegler U, Larsen S, Lundby C (2018) Exercise training increases skeletal muscle mitochondrial volume density by enlargement of existing mitochondria and not de novo biogenesis. Acta Physiol 222, e12905.

Menshikova EV, Ritov VB, Fairfull L, Ferrell RE, Kelley DE, Goodpaster BH (2006) Effects of exercise on mitochondrial content and function in aging human skeletal muscle. J Gerontol A Biol Sci Med Sci 61:534-40.

Menshikova EV, Ritov VB, Ferrell RE, Azuma K, Goodpaster BH, Kelley DE (2007) Characteristics of skeletal muscle mitochondrial biogenesis induced by moderate-intensity exercise and weight loss in obesity. J Appl Physiol (1985) 103:21-7.

Menshikova EV, Ritov VB, Toledo FG, Ferrell RE, Goodpaster BH, Kelley DE (2005) Effects of weight loss and physical activity on skeletal muscle mitochondrial function in obesity. Am J Physiol Endocrinol Metab 288:E818-25.

Miller GA (1991) The science of words. Scientific American Library New York:276 pp. Mitchell P (1961) Coupling of phosphorylation to electron and hydrogen transfer by a chemi-osmotic type of mechanism. Nature 191:144-8.

Mitchell P (1961) Coupling of phosphorylation to electron and hydrogen transfer by a chemi-osmotic type of mechanism. Nature 191:144-8.

Mitchell P (2011) Chemiosmotic coupling in oxidative and photosynthetic phosphorylation. Biochim Biophys Acta Bioenergetics 1807:1507-38.

Mitchell P, Moyle J (1967) Respiration-driven proton translocation in rat liver mitochondria. Biochem J 105:1147-62.

Mogensen M, Sahlin K, Fernström M, Glintborg D, Vind BF, Beck-Nielsen H, Højlund K (2007) Mitochondrial respiration is decreased in skeletal muscle of patients with type 2 diabetes. Diabetes 56:1592-9.

Mohr PJ, Phillips WD (2015) Dimensionless units in the SI. Metrologia 52:40-7.

Moreno M, Giacco A, Di Munno C, Goglia F (2017) Direct and rapid effects of 3,5-diiodo-L-thyronine (T2). Mol Cell Endocrinol 7207:30092-8.

Morrow RM, Picard M, Derbeneva O, Leipzig J, McManus MJ, Gouspillou G, Barbat-Artigas S, Dos Santos C, Hepple RT, Murdock DG, Wallace DC (2017) Mitochondrial energy deficiency leads to hyperproliferation of skeletal muscle mitochondria and enhanced insulin sensitivity. Proc Natl Acad Sci U S A 114:2705-10.

Nicholls DG, Ferguson S (2013) Bioenergetics. 4th edition. Elsevier.

Paradies G, Paradies V, De Benedictis V, Ruggiero FM, Petrosillo G (2014) Functional role of cardiolipin in mitochondrial bioenergetics. Biochim Biophys Acta 1837:408-17.

Pesta D, Gnaiger E (2012) High-Resolution Respirometry. OXPHOS protocols for human cells and permeabilized fibres from small biopsies of human muscle. Methods Mol Biol 810:25-58.

Pesta D, Hoppel F, Macek C, Messner H, Faulhaber M, Kobel C, Parson W, Burtscher M, Schocke M, Gnaiger E (2011) Similar qualitative and quantitative changes of mitochondrial respiration following strength and endurance training in normoxia and hypoxia in sedentary humans. Am J Physiol Regul Integr Comp Physiol 301:R1078–87.

Price TM, Dai Q (2015) The role of a mitochondrial progesterone receptor (PR-M) in progesterone action. Semin Reprod Med 33:185-94.

Prigogine I (1967) Introduction to thermodynamics of irreversible processes. Interscience, New York, 3rd ed:147pp.

Puchowicz MA, Varnes ME, Cohen BH, Friedman NR, Kerr DS, Hoppel CL (2004) Oxidative phosphorylation analysis: assessing the integrated functional activity of human skeletal muscle mitochondria – case studies. Mitochondrion 4:377-85. Puntschart A, Claassen H, Jostarndt K, Hoppeler H, Billeter R (1995) mRNAs of enzymes involved in energy metabolism and mtDNA are increased in endurance-trained athletes. Am J Physiol 269:C619-25.

Quiros PM, Mottis A, Auwerx J (2016) Mitonuclear communication in homeostasis and stress. Nat Rev Mol Cell Biol 17:213-26.

Reichmann H, Hoppeler H, Mathieu-Costello O, von Bergen F, Pette D (1985) Biochemical and ultrastructural changes of skeletal muscle mitochondria after chronic electrical stimulation in rabbits. Pflugers Arch 404:1-9.

Renner K, Amberger A, Konwalinka G, Gnaiger E (2003) Changes of mitochondrial respiration, mitochondrial content and cell size after induction of apoptosis in leukemia cells. Biochim Biophys Acta 1642:115-23.

Rich P (2003) Chemiosmotic coupling: The cost of living. Nature 421:583.

Rostovtseva TK, Sheldon KL, Hassanzadeh E, Monge C, Saks V, Bezrukov SM, Sackett DL (2008) Tubulin binding blocks mitochondrial voltage-dependent anion channel and regulates respiration. Proc Natl Acad Sci USA 105:18746-51.

Rottenberg H (1984) Membrane potential and surface potential in mitochondria: uptake and binding of lipophilic cations. J Membr Biol 81:127-38.

Rustin P, Parfait B, Chretien D, Bourgeron T, Djouadi F, Bastin J, Rötig A, Munnich A (1996) Fluxes of nicotinamide adenine dinucleotides through mitochondrial membranes in human cultured cells. J Biol Chem 271:14785-90.

Saks VA, Veksler VI, Kuznetsov AV, Kay L, Sikk P, Tiivel T, Tranqui L, Olivares J, Winkler K, Wiedemann F, Kunz WS (1998) Permeabilised cell and skinned fiber techniques in studies of mitochondrial function in vivo. Mol Cell Biochem 184:81-100.

Salabei JK, Gibb AA, Hill BG (2014) Comprehensive measurement of respiratory activity in permeabilized cells using extracellular flux analysis. Nat Protoc 9:421-38.

Sazanov LA (2015) A giant molecular proton pump: structure and mechanism of respiratory complex I. Nat Rev Mol Cell Biol 16:375-88.

Scaduto RC Jr, Grotyohann LW (1999) Measurement of mitochondrial membrane potential using fluorescent rhodamine derivatives. Biophys J 76:469-77.

Schneider TD (2006) Claude Shannon: biologist. The founder of information theory used biology to formulate the channel capacity. IEEE Eng Med Biol Mag 25:30-3.

Schönfeld P, Dymkowska D, Wojtczak L (2009) Acyl-CoA-induced generation of reactive oxygen species in mitochondrial preparations is due to the presence of peroxisomes. Free Radic Biol Med 47:503-9.

Schrödinger E (1944) What is life? The physical aspect of the living cell. Cambridge Univ Press.

Schultz J, Wiesner RJ (2000) Proliferation of mitochondria in chronically stimulated rabbit skeletal muscle--transcription of mitochondrial genes and copy number of mitochondrial DNA. J Bioenerg Biomembr 32:627-34.

Simson P, Jepihhina N, Laasmaa M, Peterson P, Birkedal R, Vendelin M (2016) Restricted ADP movement in cardiomyocytes: Cytosolic diffusion obstacles are complemented with a small number of open mitochondrial voltage-dependent anion channels. J Mol Cell Cardiol 97:197-203.

Stucki JW, Ineichen EA (1974) Energy dissipation by calcium recycling and the efficiency of calcium transport in rat-liver mitochondria. Eur J Biochem 48:365-75.

Tonkonogi M, Harris B, Sahlin K (1997) Increased activity of citrate synthase in human skeletal muscle after a single bout of prolonged exercise. Acta Physiol Scand 161:435-6.

Waczulikova I, Habodaszova D, Cagalinec M, Ferko M, Ulicna O, Mateasik A, Sikurova L, Ziegelhöffer A (2007) Mitochondrial membrane fluidity, potential, and calcium transients in the myocardium from acute diabetic rats. Can J Physiol Pharmacol 85:372-81.

Wagner BA, Venkataraman S, Buettner GR (2011) The rate of oxygen utilization by cells. Free Radic Biol Med 51:700-712.

2026  Wang H, Hiatt WR, Barstow TJ, Brass EP (1999) Relationships between muscle mitochondrial DNA content,
2027     mitochondrial enzyme activity and oxidative capacity in man: alterations with disease. Eur J Appl Physiol
2028     Occup Physiol 80:22-7.
2029  Wang T (2010) Coulomb force as an entropic force. Phys Rev D 81:104045.
2030  Watt IN, Montgomery MG, Runswick MJ, Leslie AG, Walker JE (2010) Bioenergetic cost of making an
2031     adenosine triphosphate molecule in animal mitochondria. Proc Natl Acad Sci U S A 107:16823-7.
2032  Weibel ER, Hoppeler H (2005) Exercise-induced maximal metabolic rate scales with muscle aerobic capacity. J
2033     Exp Biol 208:1635–44.
2034  White DJ, Wolff JN, Pierson M, Gemmell NJ (2008) Revealing the hidden complexities of mtDNA inheritance.
2035     Mol Ecol 17:4925–42.
2036  Wikström M, Hummer G (2012) Stoichiometry of proton translocation by respiratory complex I and its
2037     mechanistic implications. Proc Natl Acad Sci U S A 109:4431-6.
2038  Willis WT, Jackman MR, Messer JI, Kuzmiak-Glancy S, Glancy B (2016) A simple hydraulic analog model of
2039     oxidative phosphorylation. Med Sci Sports Exerc 48:990-1000.